Bachelor Project

Czech
Technical
University
in Prague

**F3**

Faculty of Electrical Engineering
Department of Control Engineering

# Vehicle electronic stabilization system development

**Lukáš Halaška**

Supervisor: Ing. Tomáš Haniš, Ph.D.
Field of study: Cybernetics and Robotics
May 2020

# BACHELOR‘S THESIS ASSIGNMENT

## I. Personal and study details

Student's name: **Halaška Lukáš** Personal ID number: **474730**

Faculty / Institute: **Faculty of Electrical Engineering**

Department / Institute: **Department of Control Engineering**

Study program: **Cybernetics and Robotics**

## II. Bachelor’s thesis details

Bachelor’s thesis title in English:

**Vehicle electronic stabilization system development**

Bachelor’s thesis title in Czech:

**Návrh elektronického stabilizačního systému vozu**

Guidelines:

The goal of this thesis is development of Electronic Stabilization Systems for vehicle dynamics. The stabilization functionality will be based on anti-symmetric braking action. The thesis will address following points:

1. Review of existing vehicle stabilization systems
2. Implementation of twin-track model for purposes of algorithms development and validation
3. Development of stabilization systems
4. Validation and testing

Bibliography / sources:

[1] Dieter Schramm, Manfred Hiller, Roberto Bardini – Vehicle Dynamics – Duisburg 2014
[2] Hans B. Pacejka - Tire and Vehicle Dynamics – The Netherlands 2012
[3] Franklin, Powell, Emami-Naeini: Feedback Control of Dynamics Systems. Prentice Hall, USA
[4] Robert Bosch GmbH - Bosch automotive handbook - Plochingen, Germany : Robert Bosch GmbH ; Cambridge, Mass. :Bentley Publishers

Name and workplace of bachelor’s thesis supervisor:

**Ing. Tomáš Haniš, Ph.D., Department of Control Engineering, FEE**

Name and workplace of second bachelor’s thesis supervisor or consultant:

Date of bachelor’s thesis assignment: **10.02.2020** Deadline for bachelor thesis submission: **22.05.2020**

Assignment valid until: **30.09.2021**

| | | |
|---|---|---|
| Ing. Tomáš Haniš, Ph.D. | prof. Ing. Michael Šebek, DrSc. | prof. Mgr. Petr Páta, Ph.D. |
| Supervisor’s signature | Head of department’s signature | Dean’s signature |

## III. Assignment receipt

The student acknowledges that the bachelor’s thesis is an individual work. The student must produce his thesis without the assistance of others, with the exception of provided consultations. Within the bachelor’s thesis, the author must state the names of consultants and include a list of references.

.

| | |
|---|---|
| Date of assignment receipt | Student’s signature |

© ČVUT v Praze, Design: ČVUT v Praze, VIC

# Acknowledgements

First, I would like to thank my supervisor Ing. Tomáš Haniš, Ph.D. for his guidance, advices, great amount of support and patience throughout the entire bachelor's project.

I would also like to express my gratitude to Ing. Vít Cibulka for providing me his twin track vehicle model as a baseline for my thesis.

Finally, I wish to thank my friends and family for their everlasting love and moral support. Without their help, not just the studies but also the life itself would be much harder.

# Declaration

I declare that the presented work was developed independently and that I have listed all sources of information used within it in accordance with the methodical instructions for observing the ethical principles in the preparation of university theses.

In Prague, 21. May 2020

# Abstract

With respect to great progress in autonomous driving technologies, modern vehicles have inbuilt a wide variety of electronic control systems, which significantly improve traffic safety. One of them is electronic stabilization system that ensures keeping the car on the right track even in unpredictable situations, such as driving on icy road or abrupt maneuvers on a highway. The purpose of this thesis was to develop such a system for created vehicle model in Simulink. The work consists of creating or modifying three vehicle models and development of two different automatic control systems. Whereas kinematic model and lookup tables are used for generating reference signals, twin track vehicle model, which the control systems are designed for, serves as a representation of a real car. As for the controllers, first method is based on principles of electronic stability program, also known as ESP, and the second strategy is enhanced stability control, abbreviated as ESC. Lastly, their functionality is experimentally validated.

**Keywords:** electronic stability program, enhanced stability control, linear control, vehicle models, vehicle dynamics, vehicle stability

**Supervisor:** Ing. Tomáš Haniš, Ph.D.
České vysoké učení technické v Praze,
Fakulta elektrotechnická,
Katedra řídicí techniky - K13135,
Karlovo náměstí 13,
12135 Praha 2

# Abstrakt

S ohledem na význačný pokrok technologií autonomního řízení mají moderní vozidla ve své výbavě širokou škálu elektronických řídících systémů, které významně zlepšují bezpečnost dopravy. Jedním z nich je elektronický stabilizační systém, jenž zajišťuje udržování automobilu ve správném směru i v nevyzpytatelných situacích, jako například při jízdě na zledovatělé cestě či při náhlých manévrech na dálnici. Smyslem této práce bylo takovýto systém navrhnout pro vytvořený model vozu v Simulinku. Práce se skládá z vytvoření či modifikace tří modelů vozu a vývoje dvou různých automatických řídících systémů. Zatímco kinematický model a vyhledávací tabulky jsou použity pro generování referenčních signálů, dvoustopý model vozu, pro nějž jsou řídící systémy navrhovány, slouží jakožto reprezentace reálného automobilu. Co se týče regulátorů, první metoda je založena na principech elektronického stabilizačního programu, také známého jako ESP, a druhou strategií je vylepšený stabilizační systém, označovaný zkratkou ESC. Nakonec je jejich funkčnost experimentálně ověřena.

**Klíčová slova:** elektronický stabilizační program, vylepšený stabilizační systém, lineární řízení, modely vozidel, dynamika vozidla, stabilita vozidla

**Překlad názvu:** Návrh elektronického stabilizačního systému vozu

# Contents

**1 Introduction 1**

**2 Vehicle dynamics models 3**

2.1 Twin track vehicle model . . . . . . . 4

2.1.1 Tire model . . . . . . . . . . . . . . . . . 5

2.1.2 Vehicle body . . . . . . . . . . . . . . . 8

2.1.3 Powertrain . . . . . . . . . . . . . . . . . 9

2.1.4 Actuators . . . . . . . . . . . . . . . . . . 10

2.1.5 Cruise control . . . . . . . . . . . . . 12

2.2 Reference models . . . . . . . . . . . . . 13

2.2.1 Kinematic vehicle model . . . . 13

2.2.2 Vehicle dynamics represented by lookup tables . . . . . . . . . . . . . . . 15

**3 Stabilization system development 19**

3.1 Reference signal selector . . . . . . . 19

3.2 Electronic stability program . . . . 20

3.3 Enhanced stability control . . . . . 22

**4 Experimental results 25**

4.1 Vehicle with ESP only . . . . . . . . . 27

4.2 Vehicle with ESP and CC . . . . . . 30

4.3 Vehicle with ESC . . . . . . . . . . . . . 33

4.4 Final comparison . . . . . . . . . . . . . 36

**5 Conclusions 39**

**A Bibliography 41**

**B Abbreviations 43**

**C Nomenclature 45**

**D Lists of vehicle parameters 47**

# Figures

2.1 Diagram of the twin track model. Adopted from [2] and modified. The dashed orange boxes mark directly modified parts. . . . . . . . . . . . . . . . . . . 4

2.2 Coordinate system of the $i$-th wheel. Adopted from [2]. . . . . . . . . . . 5

2.3 Tire traction ellipse. In the used tire model, $F_{x,max} = 4300\,\mathrm{N}$ and $F_{y,max} = 3900\,\mathrm{N}$ was considered. . . . 7

2.4 Validation of disturbance in form of changing the friction coefficient $\mu$ for both left wheels. . . . . . . . . . . . . . . 8

2.5 Validation of disturbance in form of yaw moment $M_{aero,z}$ caused by the crosswind gust. . . . . . . . . . . . . . . . . . . 9

2.6 Saturation of demanded drive torques and regenerative braking torques. . . . . . . . . . . . . . . . . . . . . . . 11

2.7 Implementation of CC. . . . . . . . 12

2.8 Control diagram of CC. . . . . . . 12

2.9 Validation of CC funcionality. The demanded drive torque is the same for each wheel. . . . . . . . . . . . . . . . . . 13

2.10 Kinematic vehicle model. Adopted from [9]. . . . . . . . . . . . . . . . 14

2.11 Lookup table data for yaw rate reference. The values of yaw rate for higher input speed and steering angle forming the dark blue plateau are the outputs of the interrupted simulations. Here, they are set to zero for better visualization, otherwise they are set to $-5$ to be well distinguished from the others. 16

2.12 Lookup table data for vehicle sideslip angle reference. The meaning of the values on the dark green plateau is explained in 2.11. . . . . . . 16

2.13 Implementation of reference model consisting of lookup tables. . 17

3.1 Control diagram of the reference signal selector. . . . . . . . . . . . . . . . . . 20

3.2 Principle of ESP. For given generated yaw moment $M_z$ brake torque is applied to the wheels of the same color. . . . . . . . . . . . . . . . . . . . . . 21

3.3 Implementation of ESP. . . . . . . 21

3.4 Control diagram of ESP. . . . . . . . 22

3.5 Illustration of speed transformation. . . . . . . . . . . . . . . . . . 23

3.6 Implementation of ESC. It is designed to work for all wheels at once. . . . . . . . . . . . . . . . . . . . . . . . . . . 24

3.7 Control diagram of ESC. . . . . . 24

4.1 Steering angle input during the maneuver. . . . . . . . . . . . . . . . . . . . . . 26

4.2 Theoretical regions of tire forces. Red line corresponds to uncontrolled vehicle, blue half circle to vehicle with ESP only and green circle covering the traction ellipse to vehicle with ESC. . . . . . . . . . . . . . . . . . . . . . 26

4.3 Performance of vehicle with ESP only compared to that of uncontrolled vehicle. . . . . . . . . . . . . 27

4.4 Forces acting on each tire. Comparison of vehicle with ESP only and uncontrolled vehicle. The dashed black line is the traction ellipse (2.3) as well as in figures 4.8 and 4.12. . 28

4.5 Slip ratios. Comparison of vehicle with ESP only and uncontrolled vehicle. . . . . . . . . . . . . . . . . . . . . . . . 28

4.6 Sideslip angles. Comparison of vehicle with ESP only and uncontrolled vehicle. . . . . . . . . . . . . 29

4.7 Performance of vehicle with ESP and CC compared to that of uncontrolled vehicle. . . . . . . . . . . . . 30

4.8 Forces acting on each tire. Comparison of vehicle with ESP and CC and uncontrolled vehicle. . . . . . 31

4.9 Slip ratios. Comparison of vehicle with ESP and CC and uncontrolled vehicle. . . . . . . . . . . . . . . . . . . . . . . . 31

4.10 Sideslip angles. Comparison of vehicle with ESP and CC and uncontrolled vehicle. . . . . . . . . . . . . 32

4.11 Performance of vehicle with ESC compared to that of uncontrolled vehicle. . . . . . . . . . . . . . . . . . . . . . . . 33

4.12 Forces acting on each tire. Comparison of vehicle with ESC and uncontrolled vehicle. . . . . . . . . . . . . 34

4.13 Slip ratios. Comparison of vehicle with ESC and uncontrolled vehicle. 34

4.14 Sideslip angles. Comparison of vehicle with ESC and uncontrolled vehicle. . . . . . . . . . . . . . . . . . . . . . . . 35

4.15 Vehicle's trajectory. Comparison of vehicle with ESP only, vehicle with ESP and CC and vehicle with ESC. 36

4.16 Vehicle's yaw rate. Comparison of vehicle with ESP only, vehicle with ESP and CC and vehicle with ESC. 37

4.17 Forces acting on each tire. Comparison of vehicle with ESP only, vehicle with ESP and CC and vehicle with ESC. . . . . . . . . . . . . . . . . . . . . 38

# Tables

2.1 State variables of the twin track model. . . . . . . . . . . . . . . . . . . . . . . . . . 5

2.2 Wheel numbering and abbreviations. . . . . . . . . . . . . . . . . . . . . 5

# Chapter 1

# Introduction

Nowadays, every new car on the market has many eletronic control systems for many different purposes. The focal point of these systems is definitely safety on the road. People are not perfect, they occasionally make mistakes, but while driving a car there is not really room for any mistakes, since the consequences are usually fatal. Automatic control systems help the driver with vehicle handling in situations, which the driver would not be able to handle by himself.

One of these systems is electronic stabilization system, also known under many different commercial names like Electronic Stability Control, Eletronic Stability Program or Dynamic Stability Control depending on automobile manufacturer. The system can detect loss of steering control and resolve it by applying brake torques to wheels individually. Some of these systems can also manage engine power. This can prevent the car from oversteer or understeer, which are terms used for the car turning more or less than commanded by the driver, respectively.

The technology of electronic stabilization system is roughly thirty years old. From 1987 to 1992, the first control system of this kind called “Elektronisches Stabilitätsprogramm” (“Electronic Stability Program”, trademarked as ESP) was co-developed by Mecredes-Benz and Bosch. It was founded on anti-lock braking system (ABS), which enabled it to brake individual wheels. Even few years before that, first traction control systems (TCS) were introduced on the market, which nowadays usually serve as a secondary function of ESP. However, compared to ABS and TCS, which improve a car’s cornering performance, ESP by itself only helps to reduce the loss of steering control.

According to [4], the main components of ESP control system are sensors, namely wheel speed sensors, a brake pressure sensor, a steering wheel angle sensor, a yaw rate sensor and a lateral acceleration sensor, electronic control unit (ECU) and actuators, namely pressure modulation and engine management.

With respect to the effectivness of ESP, the American National Highway Traffic Safety Administration (NHTSA) released a study in 2006, which claims that using ESP reduces fatal single-vehicle crashes by 35 % for cars and by 67 % for SUVs. This data and also data from other studies can be seen in [3]. Concerning the regulation, ESP has been mandatory in all new passenger vehicles in the United States since 2012. In the European Union, all new cars have been required to be equipped with ESP since 2014.

The main aim of this thesis is to develop electronic stabilization system for non-linear twin track vehicle model. Two different linear control strategies are implemented. The first algorithm is based on principles of commercial electronic stability program (ESP) and serves as a benchmark. However, this system alone controls only vehicle's stability by appliyng brake torques, and thus it does not maintain longitudinal speed of the vehicle. For this reason, cruise control can be added to work alongside with ESP. The second strategy called enhanced stability control (ESC) encompasses functionality of both ESP and cruise control. This approach also avoids using two different control systems at the same time. Moreover, ESC controls torques for each wheel individually, which makes it usable only for electric or hybrid vehicles.

# Chapter 2

# Vehicle dynamics models

For the purposes of this thesis, there is the total number of three different vehicle models used. Two of them are used as reference models and the third one, twin track model 2.1, represents real car behaviour. Since the main focus of the thesis was rather controller design than vehicle modeling, I was provided an implementation of twin track model [2] as a baseline for further modifications.

The reference models were desired to be rather simple. For lower speeds kinematic vehicle model 2.2.1 was created and for higher speeds there was an aim to create a linearized single track model. Unfortunatelly, I was not able to match the single track model to the twin track model well enough within a reasonable amount of time, so it was decided for a simpler but not less effective solution. As a second reference model, a pair of two-dimensional lookup tables 2.2.2 was created, which was sufficient for the needs of this project.

Since there were two controllable inputs, namely steering angle and longitudinal speed at the vehicle's center of gravity (further just longitudinal speed at the VCG) reference, few appropriate changes had to be made in the models to still function properly.

## 2.1 Twin track vehicle model

As already mentioned, I was provided a non-linear twin track vehicle model. For this reason the derivation of the model in this thesis does not go into too much detail. Here, only some parts of the derivation are emphasized, which had the greatest influnce on the stabilization system development or which were directly modified. The full derivation of the twin track model can be found in [2], which is based on the model derivation in [10].

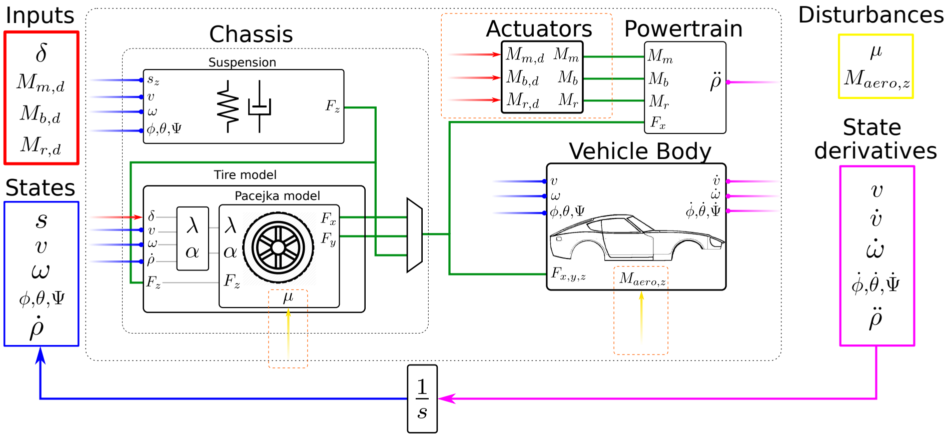
Inputs
$\delta$
$M_{m,d}$
$M_{b,d}$
$M_{r,d}$
States
$s$
$v$
$\omega$
$\phi,\theta,\Psi$
$\dot{\rho}$
Chassis
Suspension
$s_z$
$v$
$\omega$
$\phi,\theta,\Psi$
$F_z$
Tire model
Pacejka model
$\delta$
$v$
$\omega$
$\dot{\rho}$
$F_z$
$\lambda$
$\alpha$
$\lambda$
$\alpha$
$F_z$
$F_x$
$F_y$
$\mu$
Actuators
$M_{m,d}$ $M_m$
$M_{b,d}$ $M_b$
$M_{r,d}$ $M_r$
Powertrain
$M_m$
$M_b$
$M_r$
$F_x$
$\ddot{\rho}$
Vehicle Body
$v$
$\omega$
$\phi,\theta,\Psi$
$\dot{v}$
$\dot{\omega}$
$\dot{\phi},\dot{\theta},\dot{\Psi}$
$F_{x,y,z}$
$M_{aero,z}$
Disturbances
$\mu$
$M_{aero,z}$
State derivatives
$v$
$\dot{v}$
$\dot{\omega}$
$\dot{\phi},\dot{\theta},\dot{\Psi}$
$\ddot{\rho}$
$\frac{1}{s}$

**Figure 2.1:** Diagram of the twin track model. Adopted from [2] and modified. The dashed orange boxes mark directly modified parts.

The vehicle dynamics can be devided into 4 main parts, which are chassis, actuators, powertrain and vehicle body, as can be seen in figure 2.1. Here, suspension is not mentioned at all, since no modifications were done in that part. The model takes demanded drive torques, demanded brake torques and demanded regenerative braking torques for each wheel as inputs from the driver or from a control system. Additionally, it has steering angle for each wheel as an input. However, in this project the steering angle is always applied only to the front wheels having the same magnitude for both of them. The model also takes external disturbances into account. Different surfaces of the road are modeled by changing the friction coefficient $\mu$. Impact of the wind is then modeled by additional moment applied to the vehicle body.

The twin track model has 16 state variables, which are described in the following table 2.1.

| State | Unit | Desription | Dimension |
|---|---|---|---|
| $\boldsymbol{s}$ | [m] | position vector of the vehicle body (earth-fixed) | [3×1] |
| $\boldsymbol{v}$ | [m·s$^{-1}$] | vector of velocity of the vehicle body (body-fixed) | [3×1] |
| $\boldsymbol{\omega}$ | [rad·s$^{-1}$] | vector of angular velocity of the vehicle body (body-fixed) | [3×1] |
| $\phi, \theta, \psi$ | [rad] | roll, pitch, yaw (earth-fixed) | [1×1] each |
| $\dot{\rho}_i$ | [rad·s$^{-1}$] | angular speed of the $i$-th wheel (wheel-fixed) | [1×1] each |

**Table 2.1:** State variables of the twin track model.

The 4 vehicle wheels are numbered and abbreviated as follows in 2.2.

| $i$ | Wheel | Abbreviation |
|---|---|---|
| 1 | front left | FL |
| 2 | front right | FR |
| 3 | rear left | RL |
| 4 | rear right | RR |

**Table 2.2:** Wheel numbering and abbreviations.

### 2.1.1 Tire model

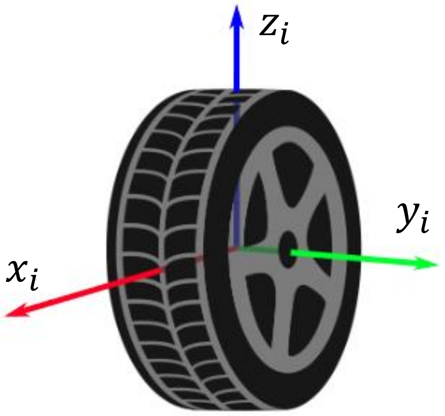

**Figure 2.2:** Coordinate system of the $i$-th wheel. Adopted from [2].

Good tire model is a crucial part of successful vehicle design, since the contact patch of a tire, which is a relatively small area, is the only part of a vehicle that directly interacts with the road surface. First there have to be defined two important variables, which are used further in tire dynamics. These are slip ratio $\lambda$ and sideslip angle $\alpha$. For each wheel they can be written as

$$\lambda_i = \frac{r\dot{\rho}_i - v_{x,i}}{\max\Big(\left|r\dot{\rho}_i\right|, \left|v_{x,i}\right|\Big)}, \tag{2.1}$$

$$\alpha_i = \arctan\left(\frac{v_{y,i}}{\left|v_{x,i}\right|}\right), \tag{2.2}$$

where $r$ is the wheel radius (for simplicity nominal radius and effective radius of the wheel are considered equal), $\dot{\rho}_i$ is angular speed of the $i$-th wheel, $v_{x,i}$ and $v_{y,i}$ are speeds of the $i$-th wheel center point along $x$ and $y$ axes, respectively. Coordinate system of the $i$-th wheel is shown in figure 2.2.

For tire to road interface modeling Pacejka Magic Formula is used. It is an empirically acquired formula by Hans Bastiaan Pacejka [8]. Parameters known as shape factors are fitted along with two inputs, which are slip ratio $\lambda$ and sideslip angle $\alpha$, into the formula creating mathematical description, which approximates characteristics of important forces and moments produced at the contact patch. These are typically longitudinal force, lateral force and aligning moment. Whereas slip ratio is used for longitudinal force calculation, lateral force and aligning moment are functions of tire sideslip angle. For given slip variable input $x$ and shape factors $B$, $C$, $D$, $E$, the formula in its most basic form calculates force $F$ as follows

$$F = D\sin\left(C\arctan\left(Bx - E(Bx - \arctan\left(Bx\right))\right)\right). \tag{2.3}$$

In this thesis, a method called “Combined slip with friction ellipse” was used, which is in detail described in [2]. This approach expresses dependency of longitudinal force and lateral force. This dependency is described by Kamm’s circle, also called traction or friction circle. Normal force $F_z$, friction coefficient $\mu$, longitudinal force $F_x$ and lateral force $F_y$ are then bound by the following inequation

$$\mu F_z \geq \sqrt{F_x^2 + F_y^2}. \tag{2.4}$$

However, in reality and also in this model an ellipse is considered instead of the circle. The ellipse is described by the inequation

$$\frac{F_x^2}{F_{x,max}^2} + \frac{F_y^2}{F_{y,max}^2} \leq 1. \tag{2.5}$$

If such $F_x$ and $F_y$ is considered that the expression on the left side of the inequation 2.5 is less than or equal to 1, the tire maintains its grip. If the expression on left side of the inequation 2.5 is greater than 1, the tire loses its grip and skids. The traction ellipse is shown in figure 2.3.

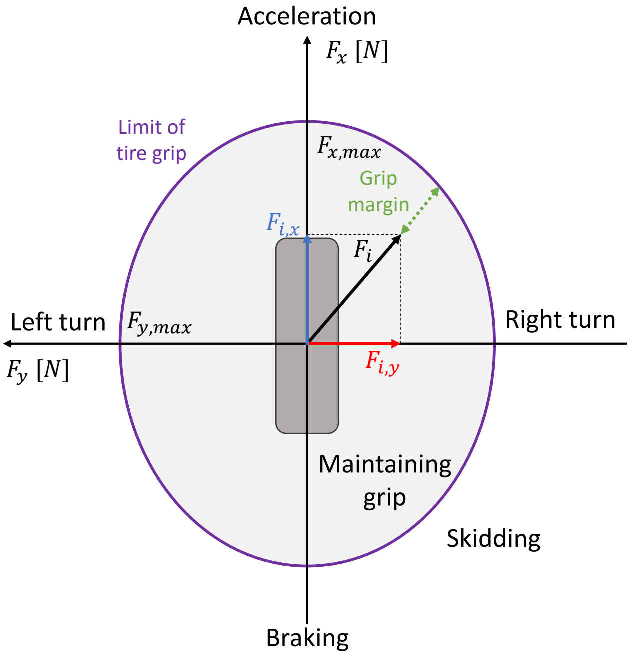

**Figure 2.3:** Tire traction ellipse. In the used tire model, $F_{x,max} = 4300\,\mathrm{N}$ and $F_{y,max} = 3900\,\mathrm{N}$ was considered.

The friction coefficient $\mu$ from the inequation 2.4 is considered to be equal to 1 under regular circumstances, which models a rather adhesive surface. Decreasing its value independently for each wheel simulates driving on slippery part of the road, which is why $\mu$ is marked as external disturbance in figure 2.1. Its impact is validated by the following simulation. The vehicle starts turning left at a constant yaw rate and at a constant longitudinal speed at the VCG. Then suddenly $\mu$ of the road surface under both left wheels is decreased to $\mu = 0.2$ resulting in decrease in the yaw rate, meaning a slight understeer. This can be seen in figure 2.4. How the twin track vehicle model maintains a constant longitudinal speed at the VCG is described in section 2.1.5.

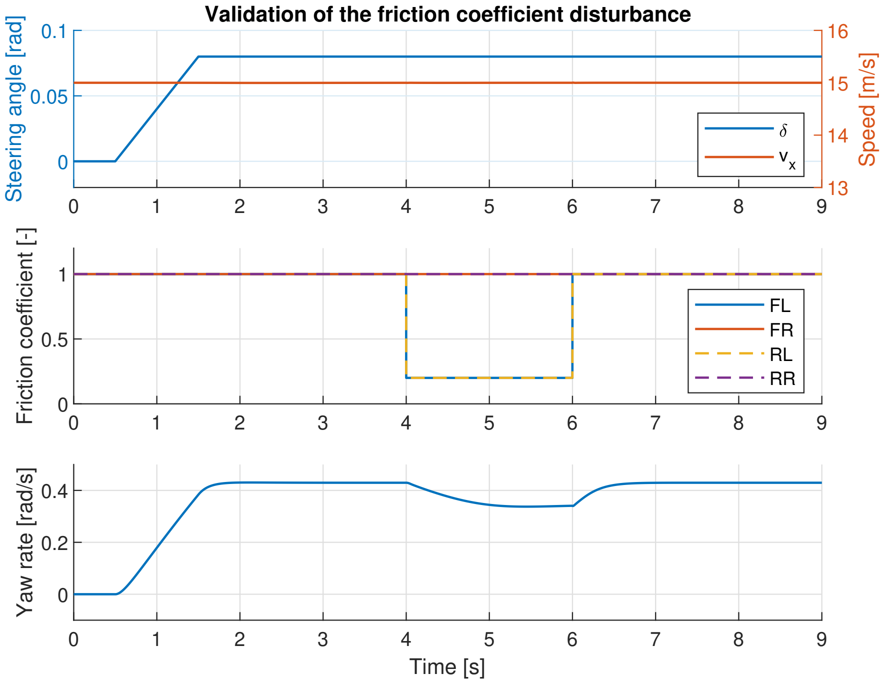

**Figure 2.4:** Validation of disturbance in form of changing the friction coefficient $\mu$ for both left wheels.

### 2.1.2 Vehicle body

Another important part of the twin track model for this thesis were equations describing the vehicle body. Since it is modeled as a rigid body, the Newton-Euler equations can be used. The important ones for the purposes of the thesis were the Euler's rotation equations, whose general vector form is

$$\boldsymbol{J}\dot{\boldsymbol{\omega}} + \boldsymbol{\omega} \times (\boldsymbol{J}\boldsymbol{\omega}) = \boldsymbol{M}, \tag{2.6}$$

where $\boldsymbol{J}$ is moment of inertia matrix of the vehicle body, $\boldsymbol{\omega}$ is vector of angular velocity of the vehicle body and $\boldsymbol{M}$ stands for vector of applied torques. The right side of the equation 2.6 can be rewritten as

$$\boldsymbol{M} = \sum_{i=1}^{4} \boldsymbol{r}_i \times \boldsymbol{F}_i + \boldsymbol{M}_{\boldsymbol{aero}}, \tag{2.7}$$

where $\boldsymbol{r}_i$ is position vector of the $i$-th wheel center point and $\boldsymbol{F}_i$ is a vector of forces applied to it. The expression $\boldsymbol{M}_{\boldsymbol{aero}}$ stands for a vector of external torques caused by aerodynamic forces. Whereas the first two elements of this vector are always considered equal to zero in this thesis, the third one $M_{aero,z}$ is a disturbance in form of external yaw moment, as can be seen in figure 2.1. Its influence is validated by the following simulation, in which the vehicle drives straight at a constant longitudinal speed at the VCG. The vehicle body then receives positive yaw moment $M_{aero,z} = 500\,\mathrm{N{\cdot}m}$ caused by the crosswind gust from the right side, which results in turning left, and so gaining positive yaw rate, as shown in figure 2.5. How the twin track model maintains a constant longitudinal speed at the VCG is described later in section 2.1.5.

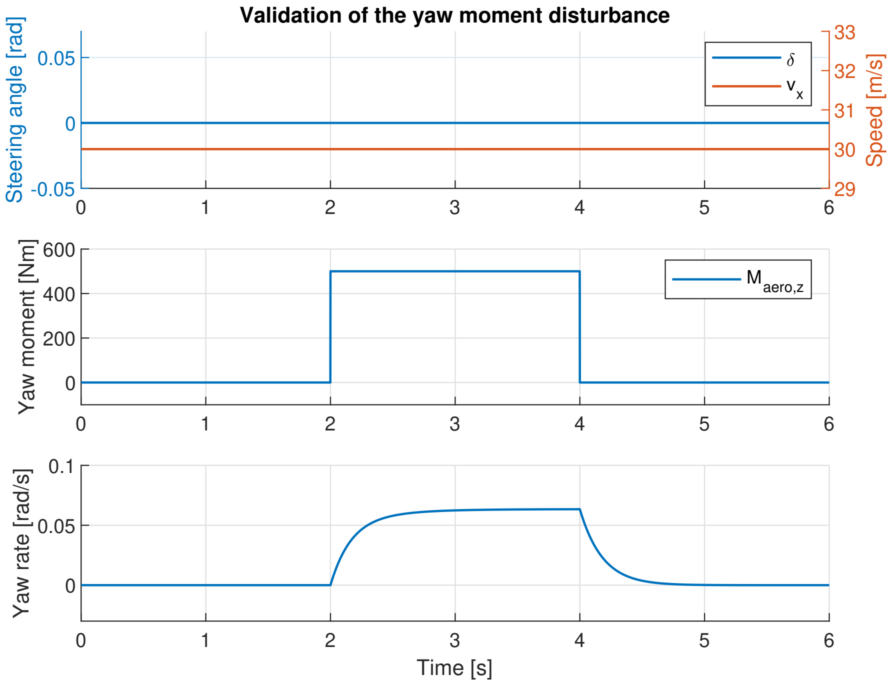

**Figure 2.5:** Validation of disturbance in form of yaw moment $M_{aero,z}$ caused by the crosswind gust.

## 2.1.3 Powertrain

Powertrain is designed so that it takes drive torques applied by the motor, brake torque and regenerative braking torque for each wheel as inputs. It is modeled by the equation

$$J_i \ddot{\rho}_i = M_{m,i} - M_{b,i} - M_{r,i} - rF_{x,i}, \tag{2.8}$$

where $J_i$ is moment of inertia of the $i$-th wheel and $\dot{\rho}_i$ is its angular speed.

$M_{m,i}$, $M_{b,i}$ and $M_{r,i}$ are drive torque, brake torque and regenerative braking torque, respectively, applied to the $i$-th wheel, $r$ is the wheel radius and $F_{x,i}$ is longitudinal force applied to the $i$-th wheel hub in its coordinate system. As only driving forward is considered for this project, each torque is always positive to satisfy the equation 2.8. Each torque's value is acquired from actuators 2.1.4.

### 2.1.4 Actuators

Implementation of actuators simulates limitations of sources of each torque from the equation 2.8. They take demanded torques from driver or from control systems as input. Each actuator consists of an input signal saturation and a tranfer function, which models a short lag.

As a source of drive toqrue the electric motor for each wheel is considered. The brushless DC motor is considered for sake of simplicity. Upper limit of saturation of demanded drive torque for the $i$-th wheel $M_{m,d,i}$ is determined either by maximum torque $M_{m,max}$ or by maximum power $P_{m,max}$ [5] depending on the $i$-th wheel angular speed $\dot{\rho}_i$, according to equation

$$M_{m,d,i} = \frac{P_{m,max}}{\dot{\rho}_i}. \tag{2.9}$$

If the speed limit of the twin track vehicle model is assumed to be $v_m = 60\,\mathrm{m{\cdot}s^{-1}}$, $P_{m,max}$ can be calculated using drag equation as follows

$$P_{m,max} = \frac{1}{2}\rho C_D A v_m^3, \tag{2.10}$$

where $\rho$ is air density, $C_D$ is the drag coefficient and $A$ is the vehicle frontal area. After plugging the values into the equation 2.10 and rounding the result, $P_{m,max} = 50\,\mathrm{kW}$ was obtained. $M_{m,max}$ was then set to $500\,\mathrm{N{\cdot}m}$. Saturation of demanded drive torques can be seen in figure 2.6.

Demanded brake torques are split into two branches if regenerative braking is used. Regenerative braking takes care of as much of the demand as it can by saturating it with its limits. The saturated signals are then substracted from the demanded brake torques, which are then fed to classic brakes. These have upper limit of saturation $M_{b,max} = 2000\,\mathrm{N{\cdot}m}$. If regenerative braking is not used, all of the demanded brake torques go straight to the classic brakes.

Regenerative braking is basically an electric motor turned into a generator. So instead of applying drive torque to a wheel, the wheel itself spins the motor, which then transforms and stores kinetic energy of the wheel. This is equivalent to applying brake torque to the wheel, as the wheel loses its kinetic energy. Regenerative braking is far more ecological than using brakes, because it not only recovers used energy, but it also does not cause environmental pollution, unlike classic brakes, which release micro-sized wear particles during braking. More on that matter can be found in [6]. Upper limit of saturation of demanded regenerative braking torques is similar to that of the DC motor, but only 40 % of $M_{m,max}$ and $P_{m,max}$ is taken into account due to its efficiency. Moreover, at low speeds the regenerative braking torque is even more limited (see [7]). Overall saturation of demanded regenerative braking torques can be seen in figure 2.6.

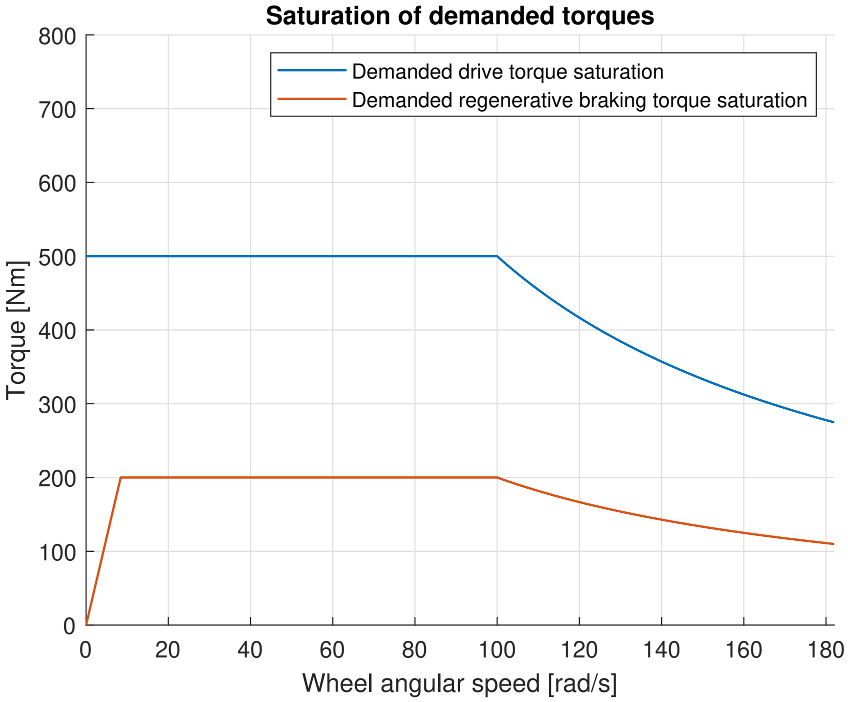

**Figure 2.6:** Saturation of demanded drive torques and regenerative braking torques.

Each actuator's lag can be modeled by a first order tranfers function [11] in form of

$$G(s) = \frac{1}{\tau s + 1}, \tag{2.11}$$

where $\tau$ is the time constant, whose magnitude expresses the delay. Since each actuator tranfers torque to torque, rather a short time constant of 2 ms was chosen for electric motors, as only the electric time constant is considered here, the mechanical time constant of powertrain is incorporated into wheel model, namely the wheel's moment of inertia. Time lag of the braking system is a bit longer, which is why its time constant was set to 20 ms.

### 2.1.5 Cruise control

Already stated in 2, longitudinal speed at the VCG reference alongside with steering angle are given inputs. However, powertrain of the twin track vehicle model defined in 2.1.3 takes drive torques as inputs. To solve this issue, cruise control had to be designed. Although this system is not directly part of the twin track model, it played an important role in formation of the lookup tables 2.2.2, which is why it is mentioned here. Cruise control (further just CC) is a system that automatically controls the speed of a vehicle by increasing or reducing drive torque applied to wheels. It is a simple feedback control system, which takes measured longitudinal speed at the VCG of the twin track model and substracts it from input speed reference. The error signal is then fed to a PI controller with anti-windup and output saturation with lower limit equal to zero and infinite upper limit. Output of the controller are the demanded drive torques. The Simulink implementation of CC can be seen in 2.7.

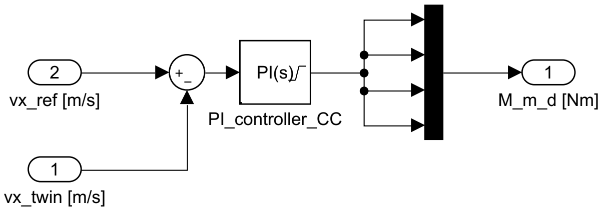

**Figure 2.7:** Implementation of CC.

Control diagram of CC is shown in 2.8.

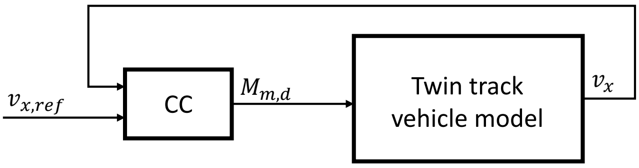

**Figure 2.8:** Control diagram of CC.

Functionality of CC is validated by the following simulation, in which the vehicle turns right while maintaining constant longitudinal speed at the VCG thanks to demands for drive torque generated by CC, as shown in figure 2.9.

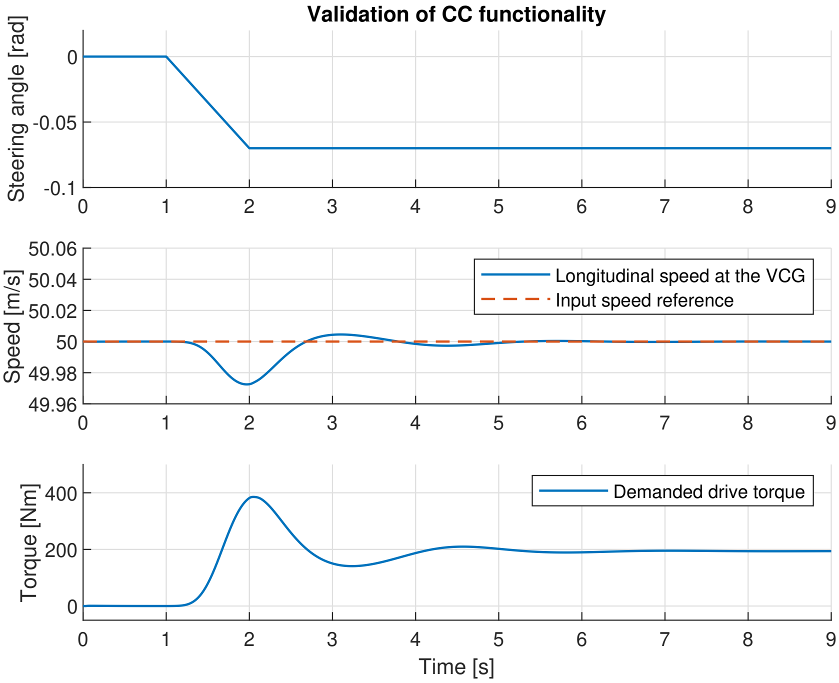

**Figure 2.9:** Validation of CC funcionality. The demanded drive torque is the same for each wheel.

## 2.2 Reference models

The purpose of reference models is to generate reference signals, which are used in electronic stabilization system. Both reference models were designed to generate yaw rate reference $\dot{\psi}_{ref}$ and vehicle sideslip angle reference $\beta_{ref}$. However, in the end only the yaw rate reference was used for development of the control systems.

### 2.2.1 Kinematic vehicle model

Kinematic vehicle model is fairly simple, yet it gives excellent results, when sideslip angles and slip ratios are very small, mainly at low speeds. It unites right and left wheels axle-wise. The united wheels lie in the geometric center of respective axles. The center of gravity lies on the line connecting the two wheels in a certain distance from each of them. Due to the absence of sideslip angles, the instant center of rotation always lies on the intersection of wheels' $y$-axes. Being given steering angle $\delta$ for the front wheel and longitudinal speed at the VCG $v_x$, the kinematic model, derivation of which can be found in [9], can then be described by the following equations

$$\beta = \arctan\left(\tan(\delta)\frac{l_r}{l_f + l_r}\right), \tag{2.12a}$$

$$\dot{X} = v_x \frac{\cos(\psi + \beta)}{\cos\beta}, \tag{2.12b}$$

$$\dot{Y} = v_x \frac{\sin(\psi + \beta)}{\cos\beta}, \tag{2.12c}$$

$$\dot{\psi} = \frac{v_x}{l_r} \tan\beta, \tag{2.12d}$$

because

$$v = \frac{v_x}{\cos\beta}. \tag{2.13}$$

The meaning of the rest of the symbols used in equations 2.12a - 2.13 can be easily understood by taking a look at figure 2.10.

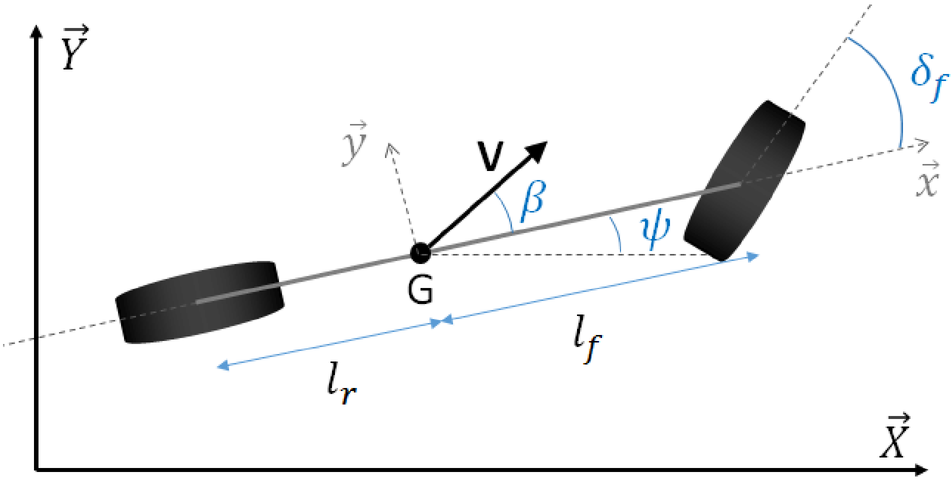

**Figure 2.10:** Kinematic vehicle model. Adopted from [9].

### 2.2.2 Vehicle dynamics represented by lookup tables

Lookup table is a data structure, which replaces a mathematical function or operation. It stores a limited and predefined set of output values corresponding to a limited and predefined set of input values. Even if the input is not from the predefined set, MATLAB lookup table can still usually provide an output using various interpolation and extrapolation methods. The extrapolation is unfortunatelly not always possible.

The lookup tables were designed as a reference model for higher speeds. To be precise, two two-dimensional lookup tables were created, one of them for generating yaw rate reference and the second one for generating vehicle sideslip angle reference. The lookup tables are two-dimensional, as steering angle and longitudinal speed at the VCG are considered as inputs, so there are two sets of input values, one for each input. Data for the lookup tables were generated by the following procedure.

Using the twin track model with CC, around nine thousand simulations were conducted. Each one was twenty seconds long and consisted of driving straight for one second and then turning left with constant steering angle $\delta$ as first input while maintaining constant longitudinal speed at the VCG $v_x$ as second input. For smoother transient response of the twin track model and also for more realistic nature of the maneuver, the used steering angle input was not actually a step function with infinitely short rising edge, but its ramp-like rising edge was two seconds long. The values for $\delta$ were in the interval $\langle 0, \frac{\pi}{9} \rangle$ rad and the values for $v_x$ were in the interval $\langle 5, 60 \rangle$ m·s$^{-1}$.

Since the lookup tables were desired to model the vehicle when its tires maintain grip (see 2.3), maximal slip ratio for peak longitudinal force and maximal sideslip angle for peak lateral force of the tire had to be estimated. After various experiments, the values were estimated to be $\lambda_{max} = 0.1$ and $\alpha_{max} = 0.35\,\text{rad}$. If any of these two values were exceeded by any wheel during the maneuver, the simulation was stopped and no output value was recorded, as it meant the vehicle started skidding. If the simulation was not interrupted in the process, the very last values of the simulation were recorded as reference outputs for corresponding inputs, as the twin track model could be considered to be in a steady state after twenty seconds. Whereas yaw rate was directly generated by the twin track model, vehicle sideslip angle had to be calculated as follows

$$\beta = \arctan\left(\frac{v_y}{|v_x|}\right), \tag{2.14}$$

where $v_x$ and $v_y$ are longitudinal and lateral speed at the VCG, respectively. The values stored in the lookup tables are shown in figures 2.11 and 2.12.

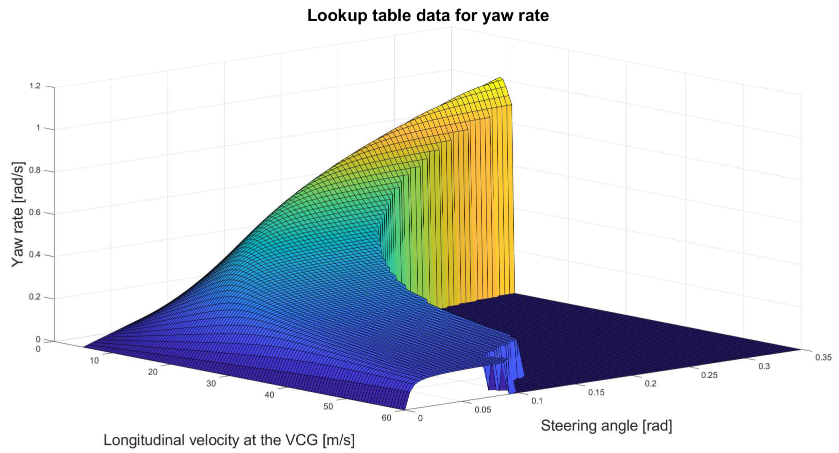

**Figure 2.11:** Lookup table data for yaw rate reference. The values of yaw rate for higher input speed and steering angle forming the dark blue plateau are the outputs of the interrupted simulations. Here, they are set to zero for better visualization, otherwise they are set to $-5$ to be well distinguished from the others.

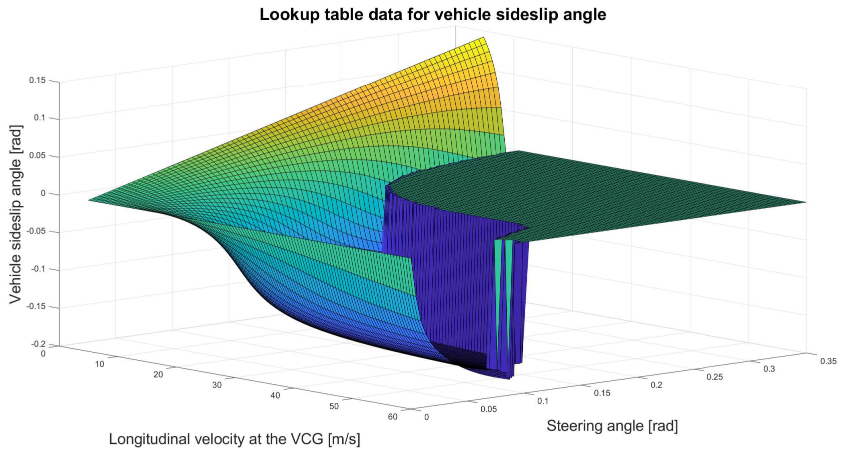

**Figure 2.12:** Lookup table data for vehicle sideslip angle reference. The meaning of the values on the dark green plateau is explained in 2.11.

The lookup table data for negative steering angle input are derived from the values for positive steering angles by simply multiplying them by $-1$, because the twin track model is symmetrical. Simulink implementation of the reference model consisting of the two lookup tables can be seen in 2.13.

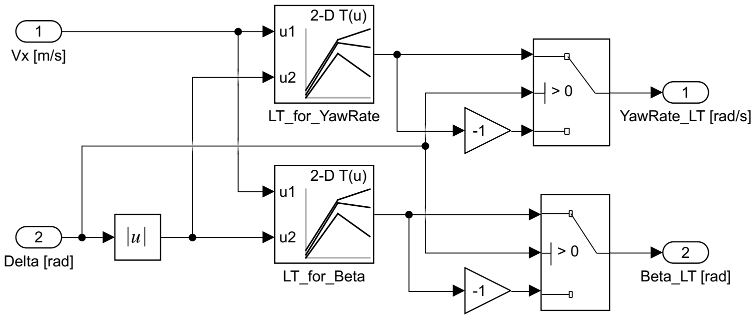
1
Vx [m/s]
2-D T(u)
u1
u2
LT_for_YawRate
> 0
1
YawRate_LT [rad/s]
-1
2
Delta [rad]
|u|
2-D T(u)
u1
u2
LT_for_Beta
> 0
2
Beta_LT [rad]
-1

**Figure 2.13:** Implementation of reference model consisting of lookup tables.

# Chapter 3

# Stabilization system development

This chapter contains a detailed description of each method of stabilization system development. First, a selector 3.1 had to be designed, which would select suitable reference signals for the control system depending on the measured speed. Then two different control algorithms were implemented. The first and also the simpler strategy is electronic stability program 3.2. The second method is enhanced stability control 3.3.

## 3.1 Reference signal selector

This selector is constructed to select appropriate set of reference signals for the control system. Besides yaw rate and vehicle sideslip angle generated by both kinematic vehicle model and lookup tables, it takes longitudinal speed at the VCG as input. Deciding by the magnitude of the measured speed from the twin track model, it selects appropriate yaw rate and vehicle sideslip reference. If the speed is less or equal to $5\,\mathrm{m{\cdot}s^{-1}}$ and greater or equal to $0\,\mathrm{m{\cdot}s^{-1}}$ at the same time, as only driving forward is considered, signals generated by the kinematic vehicle model are selected. For the measured speed higher than $5\,\mathrm{m{\cdot}s^{-1}}$, the kinematic vehicle model does not provide satisfactory results anymore, therefore signals generated by the lookup tables are selected. Nevertheless, as mentioned in 2.2, vehicle sideslip angle reference was not needed for stabilization system development in the end. Control chart of the reference signal selector can be seen in figure 3.1.

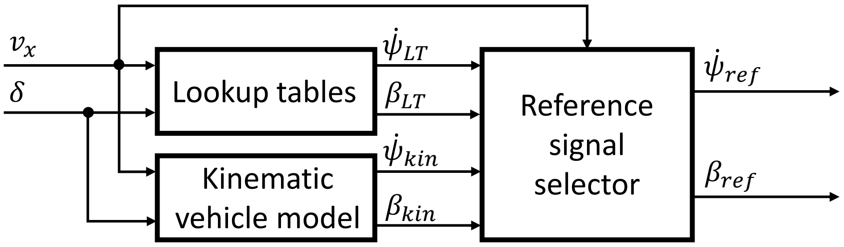

**Figure 3.1:** Control diagram of the reference signal selector.

## 3.2 Electronic stability program

The first feedback control algorithm is based on increasing or reducing yaw moment, which is done by applying brake torques either to both left wheels or to both right wheels. As yaw rate is the only measured quantity and this method can be generally implemented for vehicle with any propulsion system, regenerative braking cannot be used. Measured yaw rate from the twin track model is substracted from yaw rate reference. The difference is then fed to a P controller, whose output signal is the desired yaw moment. If the generated yaw moment is positive, then the demanded brake torques equal to this moment are applied to both left wheels. On the other hand, if the generated yaw moment is negative, then it is multiplied by $-1$, which transforms it into the demanded brake torques that are applied to both right wheels. This logic is depicted in figure 3.2 and in the implementation it is realized by the saturation blocks in figure 3.3.

Since ESP is not always active and it only intervenes when significant loss of steering control is detected, as stated in [1], a deadzone in form of a switch was added. It switches the ESP off when the absolute value of the difference between measured yaw rate and yaw rate reference is lower than $\Delta\dot{\psi}_{ESP} = 0.035\,\mathrm{rad{\cdot}s^{-1}}$ and sets the demanded brake torques to zero instead. This number was obtained empirically as a compromise between two opposing requirements. The first requirement was that the control system should react to loss of steering control in time, which minimized the value. However, lower values would cause switching the ESP too frequently, which would not be realistically possible. Also a short delay (1 ms) in form a first order transfer function was added to the switch to make it more realistic.

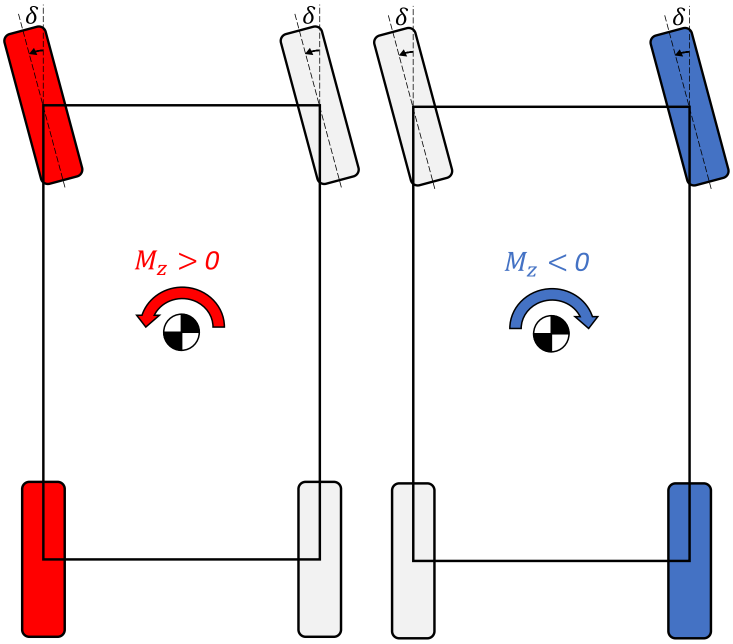
δ
δ
δ
δ
$M_z > 0$
$M_z < 0$

**Figure 3.2:** Principle of ESP. For given generated yaw moment $M_z$ brake torque is applied to the wheels of the same color.

The Simulink implementation of ESP can be seen in figure 3.3.

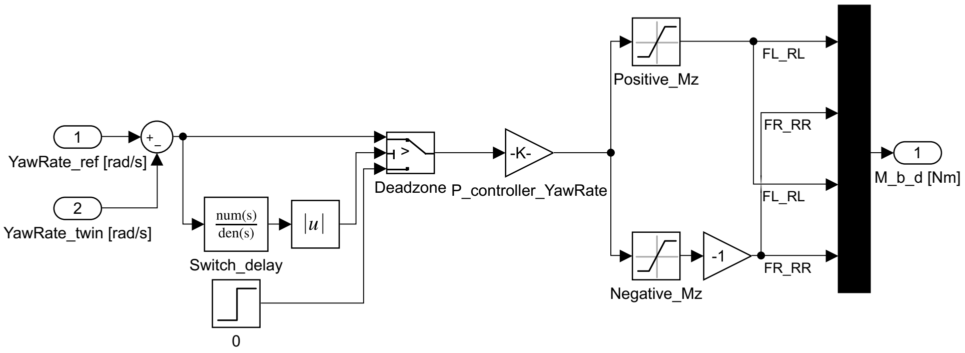
1
YawRate_ref [rad/s]
2
YawRate_twin [rad/s]
+
-
num(s)
den(s)
Switch_delay
|u|
0
>
Deadzone
-K-
P_controller_YawRate
Positive_Mz
Negative_Mz
-1
FL_RL
FR_RR
FL_RL
FR_RR
1
M_b_d [Nm]

**Figure 3.3:** Implementation of ESP.

Control diagram of ESP is shown in the following figure 3.4.

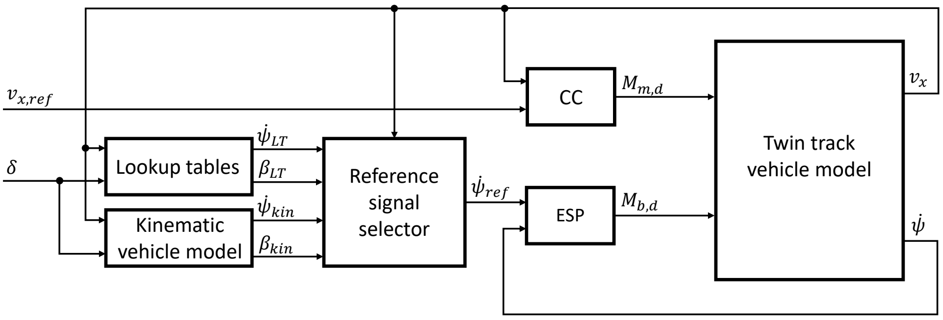
$v_{x,ref}$
$\delta$
Lookup tables
Kinematic vehicle model
$\dot{\psi}_{LT}$
$\beta_{LT}$
$\dot{\psi}_{kin}$
$\beta_{kin}$
Reference signal selector
$\dot{\psi}_{ref}$
CC
ESP
$M_{m,d}$
$M_{b,d}$
Twin track vehicle model
$v_x$
$\dot{\psi}$

**Figure 3.4:** Control diagram of ESP.

## 3.3 Enhanced stability control

The second control strategy is based on independent control of each wheel torque. In comparison to ESP 3.2, this system is always active, since it only not controls brake torques, but also drive torques. As a result, no CC is needed, as this system encompasses its functionality as well. On top of that, use of regenerative braking is made, as angular speed of each wheel is measured as well.

First, transformation of longitudinal speed at the VCG into longitudinal speed of each wheel in body-fixed frame is done. Follow-up transformation of the longitudinal speed into wheel-fixed frame is omitted as a result of simplification, since for low steering angles the transformation would have almost no impact. If ${}^{VCG}v_x$ is longitudinal speed at the VCG and ${}^{W_i}v_x$ is longitudinal speed of the $i$-th wheel in body-fixed frame, then for reference signals is

$$ {}^{W_i}v_{x,ref} = {}^{VCG}v_{x,ref} - s_l\dot{\psi}_{ref}, \tag{3.1} $$

when $i \in \{1, 3\}$ and

$$ {}^{W_i}v_{x,ref} = {}^{VCG}v_{x,ref} + s_r\dot{\psi}_{ref}, \tag{3.2} $$

when $i \in \{2, 4\}$, where $s_l$ and $s_r$ is lateral distance from the VCG to left and right wheels, respectively. The same applies to measured signals from the twin track model, if we substitute all $_{ref}$ indexes in the equations 3.1 and 3.2 with $_m$, which denotes a measured signal. This speed transformation can be understood by examining figure 3.5.

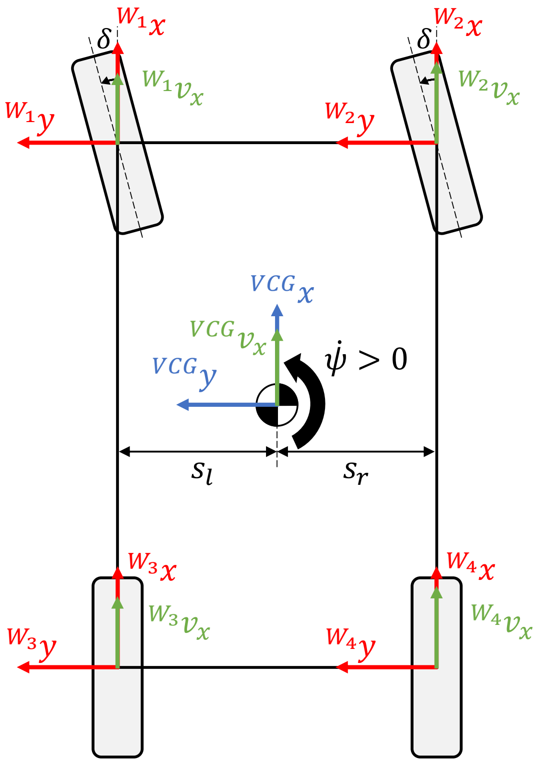

**Figure 3.5:** Illustration of speed transformation.

The following applies to each wheel. Then, $^{W_i}v_{x,m}$ is substracted from $^{W_i}v_{x,ref}$ and the difference is fed to a simple P controller, which returns slip ratio $\lambda_i$. This slip ratio is then saturated with lower limit $\lambda_{i,min} = -0.1$ and upper limit $\lambda_{i,max} = 0.1$ (values taken from 2.2.2 for the same reason). Depending on $^{W_i}v_{x,m}$ and $\dot{\rho}_{i,m}$, which is measured angular speed of the $i$-th wheel, angular speed reference is calculated for further control. The calculation is derived from the equation 2.1. If $r\dot{\rho}_{i,m} \geq {}^{W_i}v_{x,m}$ ($r$ is the wheel radius) and $^{W_i}v_{x,m} \geq 0$, then

$$\dot{\rho}_{i,ref} = \frac{^{W_i}v_{x,m}}{r(1-\lambda_i)}. \tag{3.3}$$

On the contrary, if $r\dot{\rho}_{i,m} < {}^{W_i}v_{x,m}$ and $^{W_i}v_{x,m} \geq 0$, then

$$\dot{\rho}_{i,ref} = \frac{^{W_i}v_{x,m}(1+\lambda_i)}{r}. \tag{3.4}$$

Since only driving forward is considered, equations for $^{W_i}v_{x,m} < 0$ are not explicitly stated here. However, they both only differ in the used plus and minus sign, compared to the equations 3.3 and 3.4. Measured angular speed of each wheel is then substracted from its generated reference. Once again, usage of a P controller was sufficient for the closed-loop control. If the output signal of the controller is positive, it stands for the demanded drive torque. On the other hand, if the output signal is negative, it is the demanded brake torque, which is the reason, why the signal is multiplied by $-1$ before being sent to regenerative braking system and brakes.

The Simulink implementation of ESC can be seen in figure 3.6.

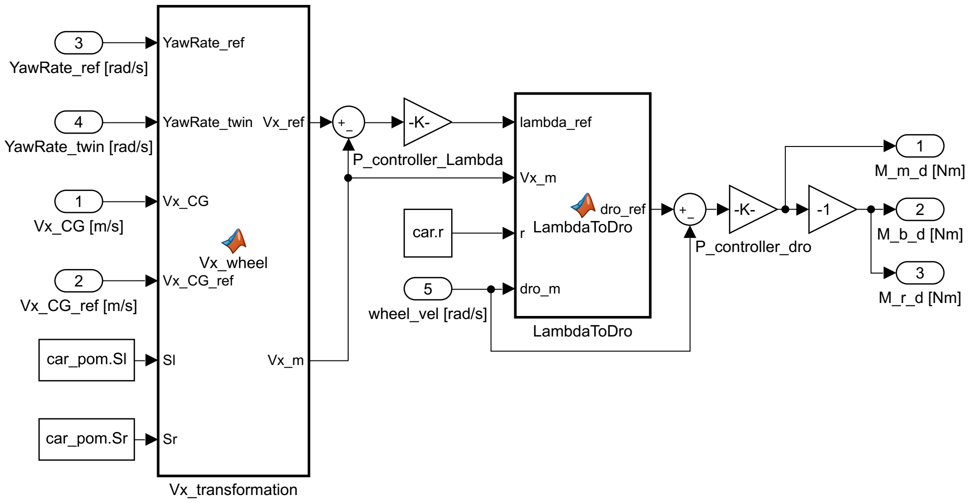
3
YawRate_ref [rad/s]
4
YawRate_twin [rad/s]
1
Vx_CG [m/s]
2
Vx_CG_ref [m/s]
car_pom.Sl
car_pom.Sr
YawRate_ref
YawRate_twin
Vx_ref
Vx_CG
Vx_wheel
Vx_CG_ref
Sl
Vx_m
Sr
Vx_transformation
+
_
-K-
P_controller_Lambda
lambda_ref
Vx_m
car.r
r
dro_ref
LambdaToDro
5
wheel_vel [rad/s]
dro_m
LambdaToDro
+
_
-K-
P_controller_dro
-1
1
M_m_d [Nm]
2
M_b_d [Nm]
3
M_r_d [Nm]

**Figure 3.6:** Implementation of ESC. It is designed to work for all wheels at once.

Control chart of ESC is shown in figure 3.7.

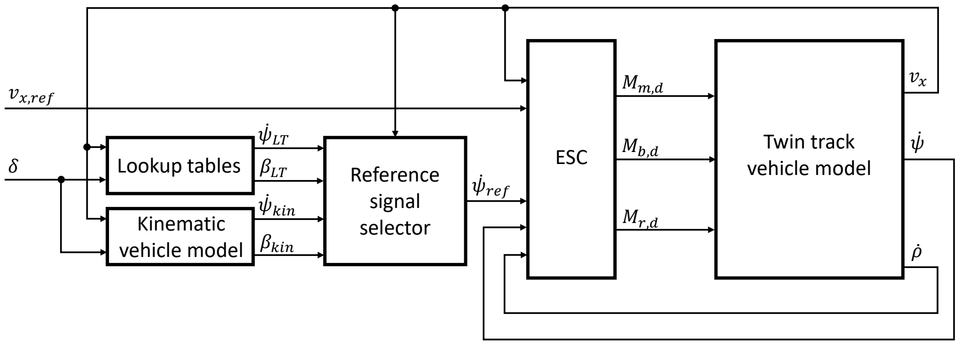
$v_{x,ref}$
$\delta$
Lookup tables
Kinematic vehicle model
$\dot{\psi}_{LT}$
$\beta_{LT}$
$\dot{\psi}_{kin}$
$\beta_{kin}$
Reference signal selector
$\dot{\psi}_{ref}$
ESC
$M_{m,d}$
$M_{b,d}$
$M_{r,d}$
Twin track vehicle model
$v_x$
$\dot{\psi}$
$\dot{\rho}$

**Figure 3.7:** Control diagram of ESC.

# Chapter 4

# Experimental results

This part shows results of an experiment, which was conducted to validate functionality of the developed stabilization systems. This experiment simulates a steering maneuver on a highway. The driver tries to avoid an obstacle suddenly appearing in front of him, which represents a car crash or an abruptly braking car. This causes the driver to quickly change the steering angle. Considering high initial longitudinal speed at the VCG, namely $v_x = 35\,\mathrm{m{\cdot}s^{-1}}$, this maneuver generates a significant action on vehicle lateral dynamics, which can result in loss of steering control. The following steering angle input 4.1 is considered for the maneuver.

First, results of vehicle with three different control system configurations are presented separately, each in comparison with uncontrolled vehicle. The three configurations are vehicle with ESP only, vehicle with ESP and CC and vehicle with ESC. These three are then compared with each other. Since ESP alone only applies brake torques and ESC controls all wheel torques, it can be predicted that the force acting on the contact patch of each tire during the entire experiment can only be part of a corresponding area of the traction ellipse marked in figure 4.2. Nevertheless, uncontrolled vehicle is considered to have CC always active for this experiment, which is the reason, why the area corresponding to it in figure 4.2 actually slightly expands to the upper half-plane (positive values of $F_x$).

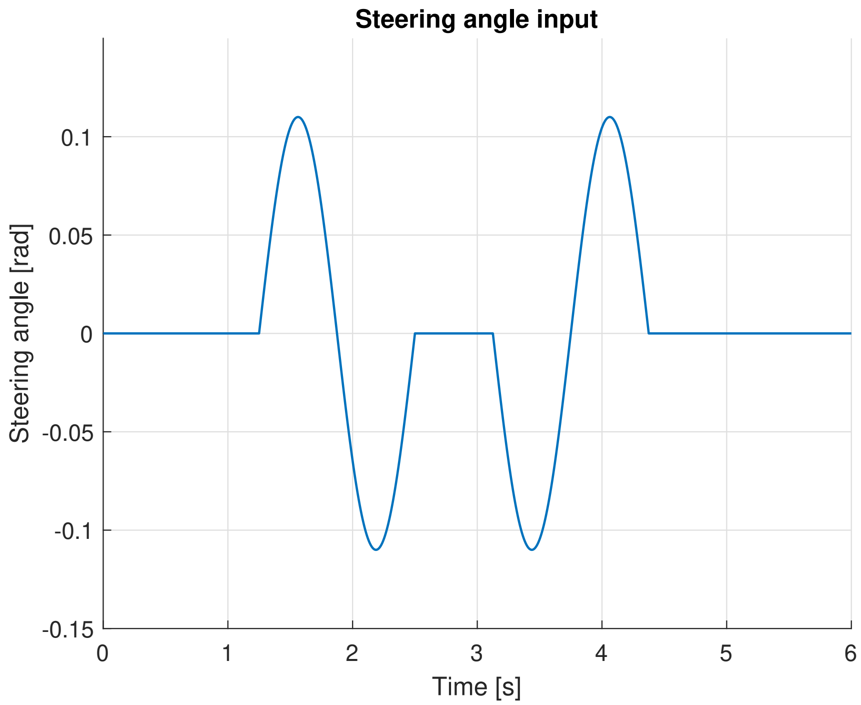

**Figure 4.1:** Steering angle input during the maneuver.

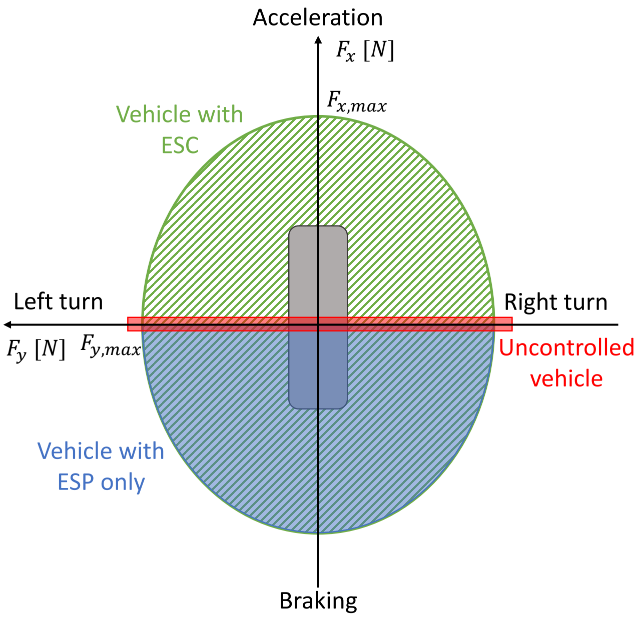
Acceleration
$F_x$ [N]
$F_{x,max}$
Vehicle with ESC
Left turn
Right turn
$F_y$ [N]
$F_{y,max}$
Uncontrolled vehicle
Vehicle with ESP only
Braking

**Figure 4.2:** Theoretical regions of tire forces. Red line corresponds to uncontrolled vehicle, blue half circle to vehicle with ESP only and green circle covering the traction ellipse to vehicle with ESC.

## 4.1 Vehicle with ESP only

As can be seen in 4.3, ESP was able to stabilize the vehicle, but the vehicle was not able to maintain its initial longitudinal speed, because only brake torques were applied. Even though the difference in yaw rate between vehicle with ESP and uncontrolled vehicle might not seem that radical at first glance, the diagram showing the vehicle's trajectory truly displays the impact of ESP. In regard to tire forces, only those ones from time interval $\langle 1.25, 1.875\rangle$ s, which corresponds to the first left turn, are shown in figure 4.4 for clarity. This applies to sections 4.2 and 4.3 as well. Forces in 4.4 confirm the prediction in 4.2. Furthermore, slip ratios and sideslip angles are shown in figures 4.5 and 4.6, respectively.

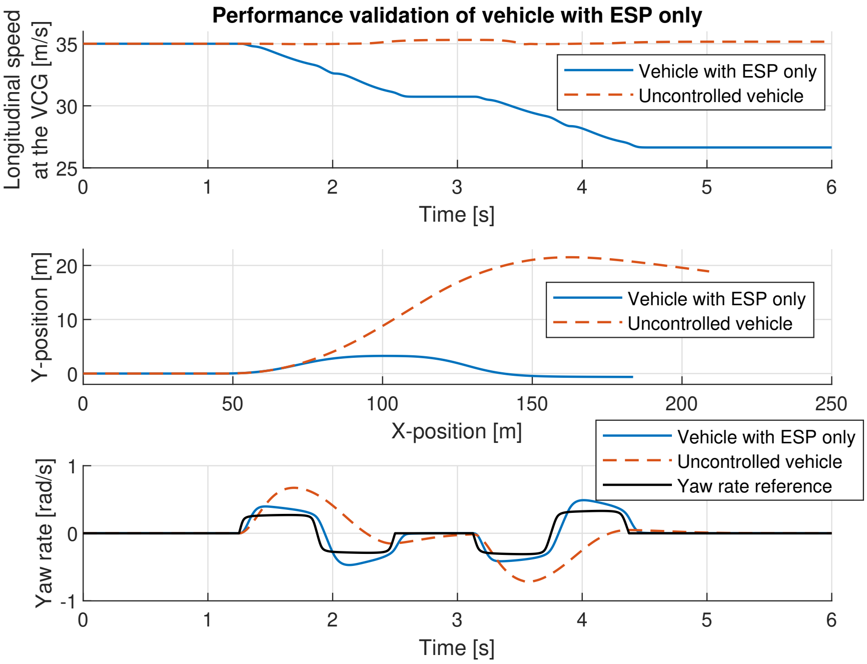

**Figure 4.3:** Performance of vehicle with ESP only compared to that of uncontrolled vehicle.

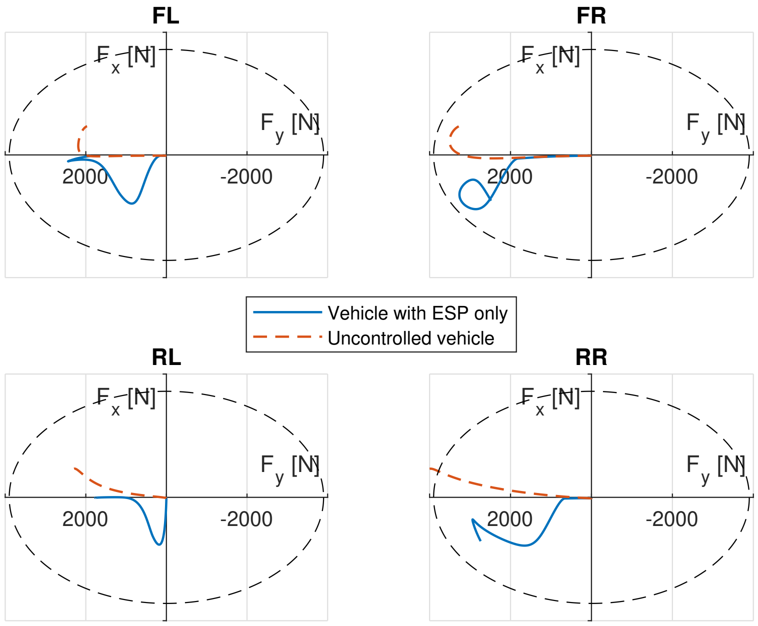

**Figure 4.4:** Forces acting on each tire. Comparison of vehicle with ESP only and uncontrolled vehicle. The dashed black line is the traction ellipse (2.3) as well as in figures 4.8 and 4.12.

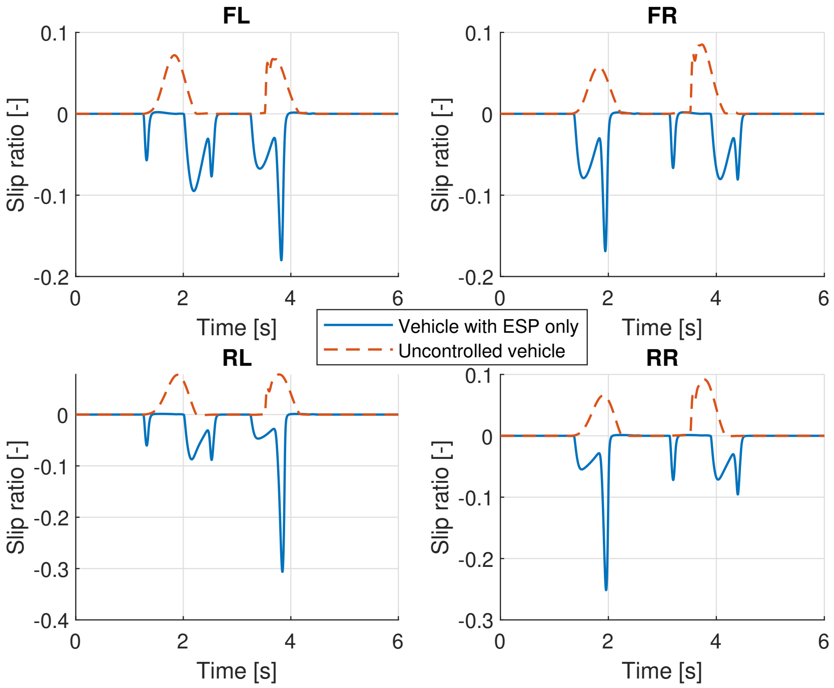

**Figure 4.5:** Slip ratios. Comparison of vehicle with ESP only and uncontrolled vehicle.

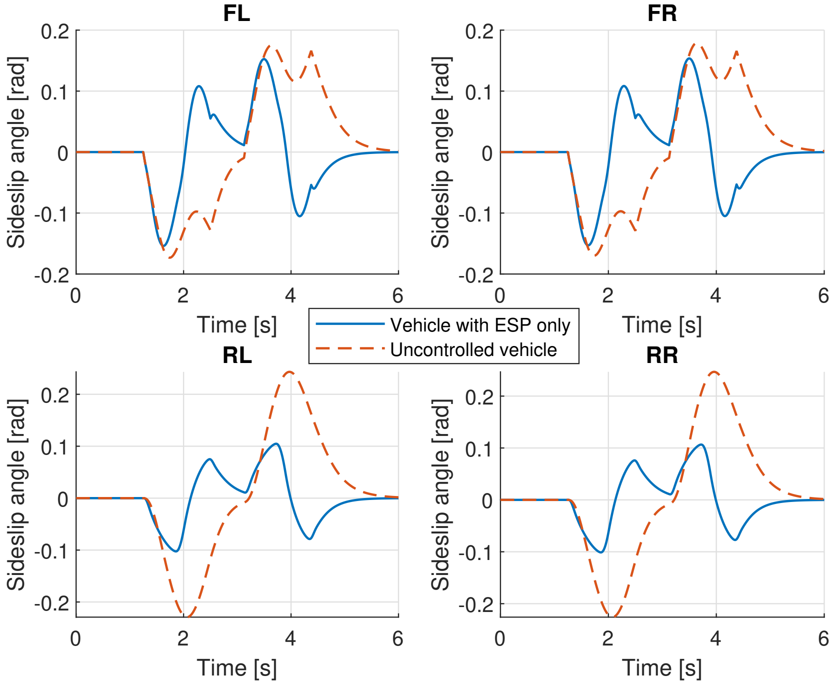

**Figure 4.6:** Sideslip angles. Comparison of vehicle with ESP only and uncontrolled vehicle.

## 4.2 Vehicle with ESP and CC

When CC is added to work alongside with ESP, initial logitudinal speed is maintained, which is shown in figure 4.7. This addition strictly goes against ESP implementation requirements, as once ESP is switched on, any other system needs to be suspended. The vehicle component management system is not considered in this work, therefore such combination of function can be investigated. With CC generating drive torques, longitudinal force $F_x$ acting on a tire can take positive values as well as negative values (caused by ESP), which can be seen in 4.8. Moreover, slip ratios and sideslip angles are shown in figures 4.9 and 4.10, respectively.

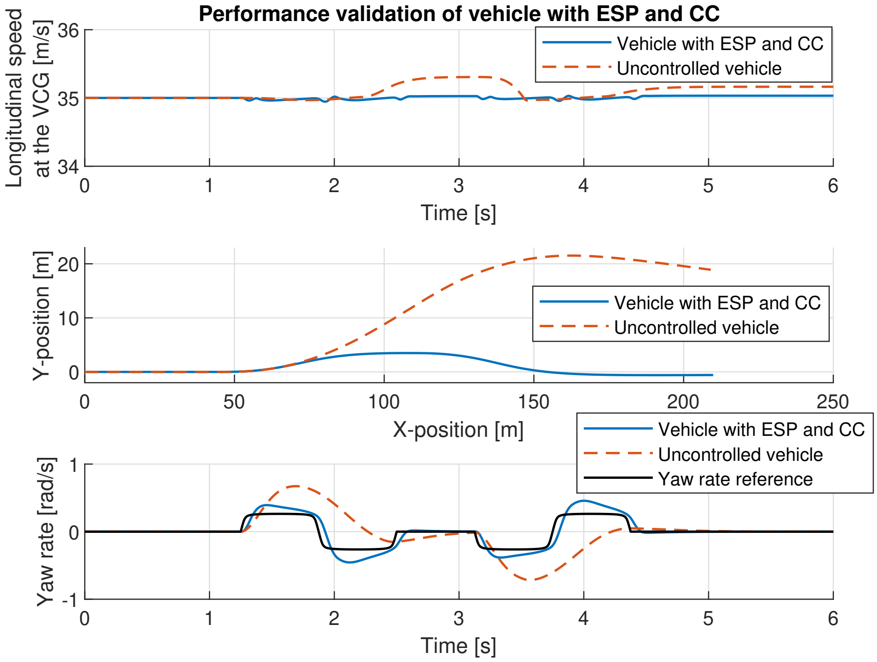

**Figure 4.7:** Performance of vehicle with ESP and CC compared to that of uncontrolled vehicle.

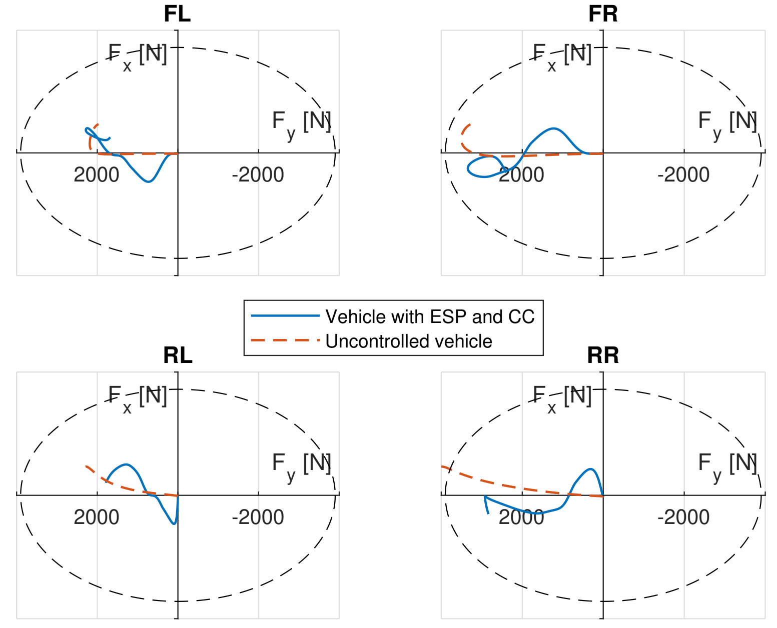

**Figure 4.8:** Forces acting on each tire. Comparison of vehicle with ESP and CC and uncontrolled vehicle.

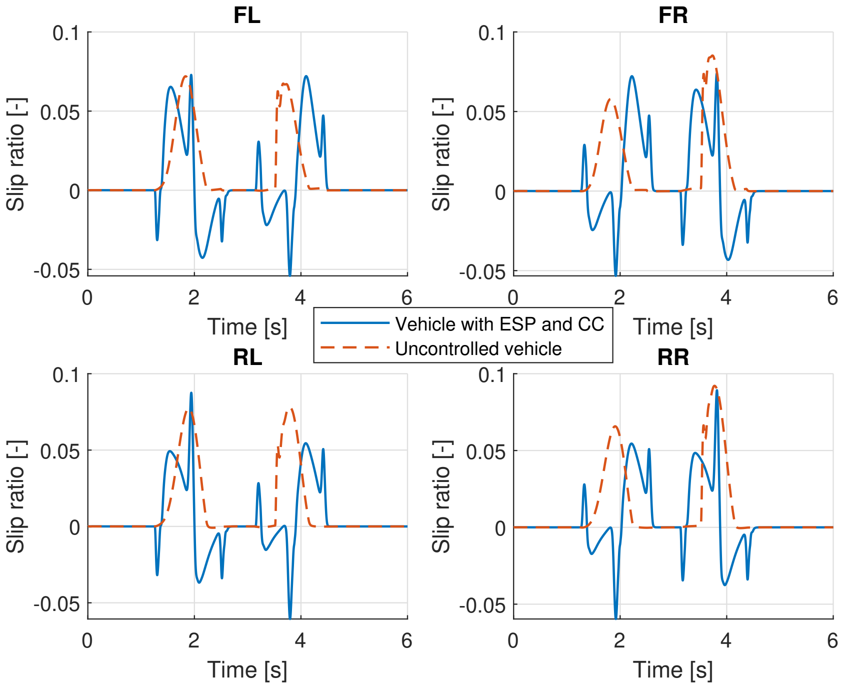

**Figure 4.9:** Slip ratios. Comparison of vehicle with ESP and CC and uncontrolled vehicle.

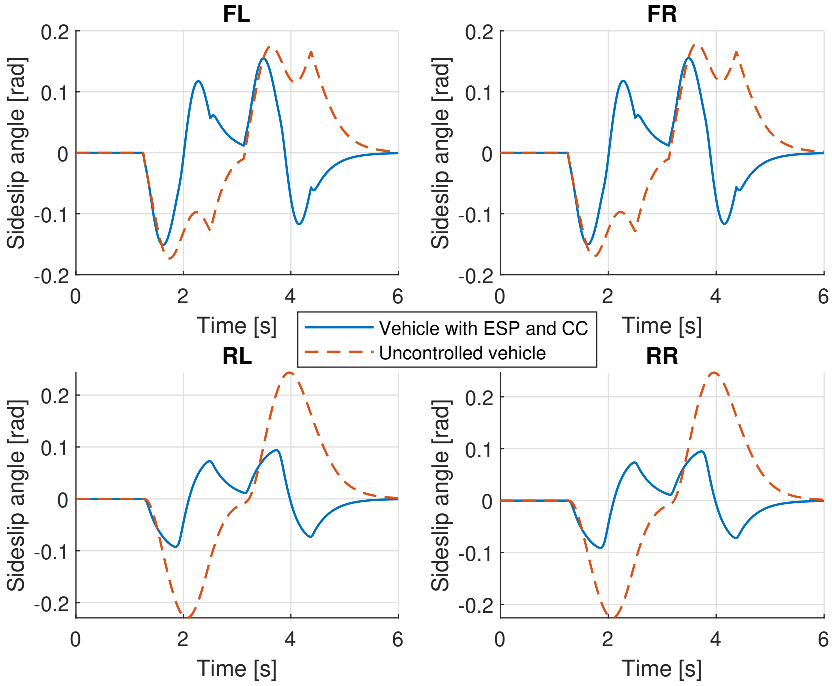

**Figure 4.10:** Sideslip angles. Comparison of vehicle with ESP and CC and uncontrolled vehicle.

## 4.3 Vehicle with ESC

As a single control system, ESC encompasses functionality of both ESP and CC. Its functionality is validated in figure 4.11. It shows, how yaw rate of vehicle with ESC almost flawlessly copies its reference. Additionally, forces in 4.12 confirm the prediction stated in 4.2. Furthermore, slip ratios and sideslip angles can be seen in figures 4.13 and 4.14, respectively.

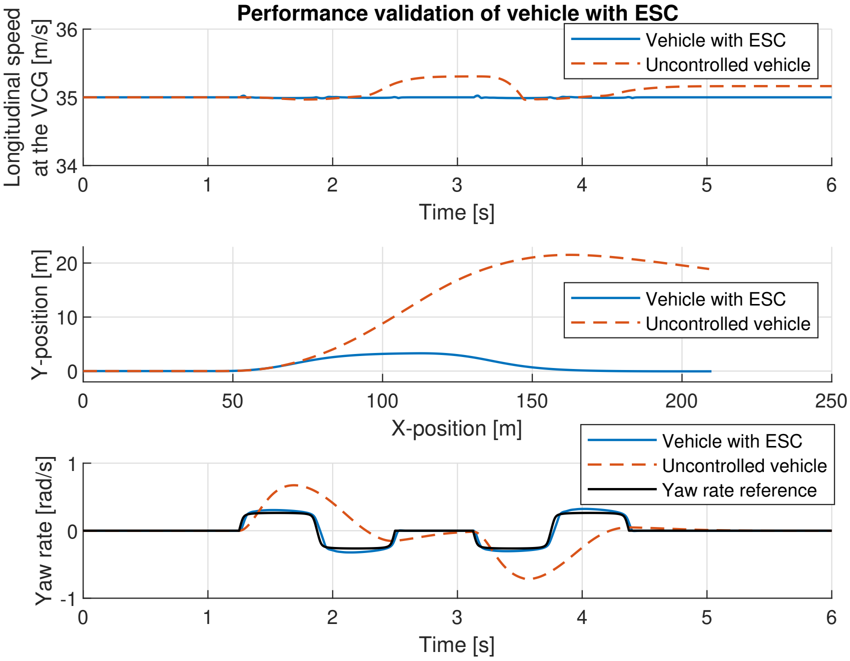

**Figure 4.11:** Performance of vehicle with ESC compared to that of uncontrolled vehicle.

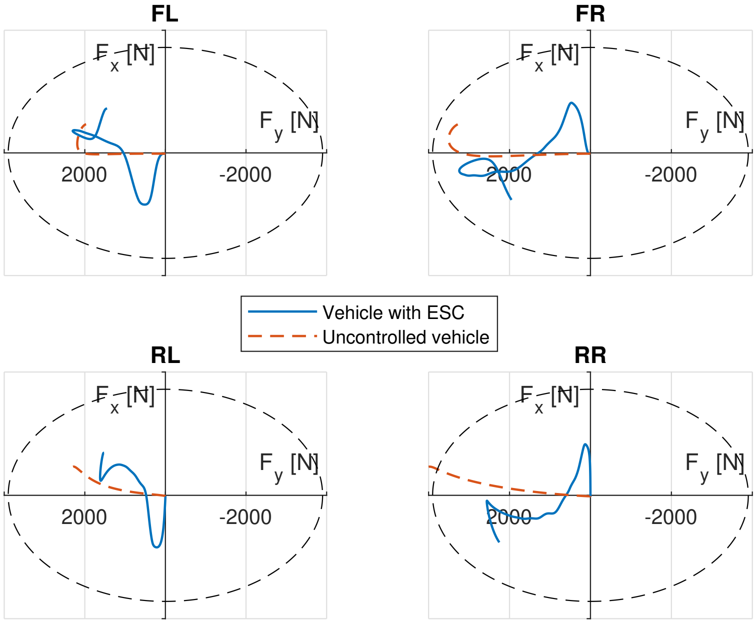

**Figure 4.12:** Forces acting on each tire. Comparison of vehicle with ESC and uncontrolled vehicle.

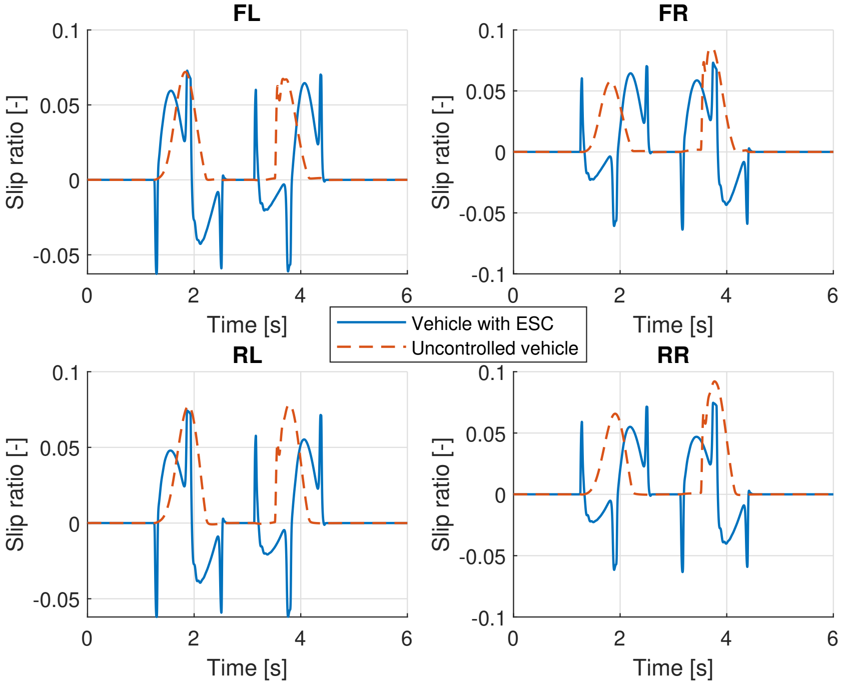

**Figure 4.13:** Slip ratios. Comparison of vehicle with ESC and uncontrolled vehicle.

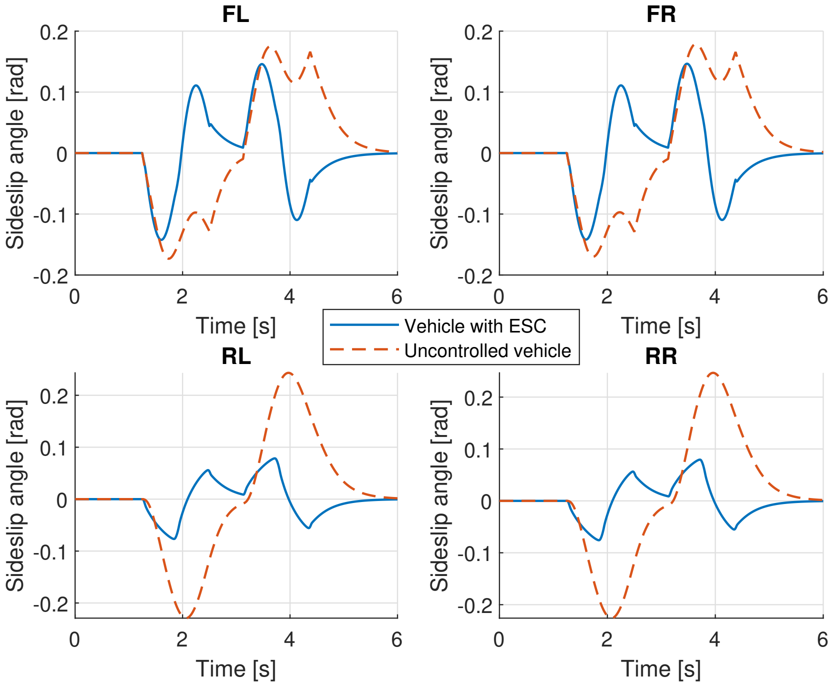

**Figure 4.14:** Sideslip angles. Comparison of vehicle with ESC and uncontrolled vehicle.

## 4.4 Final comparison

Performances of vehicle with ESP only, vehicle with ESP and CC and vehicle with ESC are compared with each other in this section. As can be seen in 4.15, all trajectories look quite similar, yet only vehicle with ESC was able to return to roughly the same $y$-postion after the maneuver, whereas vehicles with ESP were shifted more than half a meter to the right.

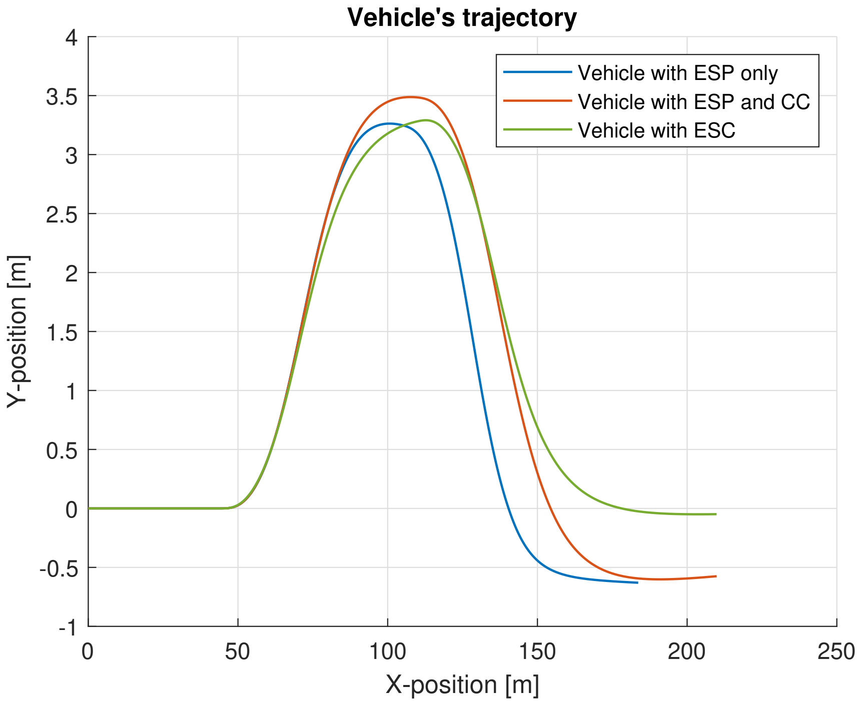

**Figure 4.15:** Vehicle's trajectory. Comparison of vehicle with ESP only, vehicle with ESP and CC and vehicle with ESC.

Regarding yaw rate, a rather small difference between vehicle with ESP only and vehicle with ESP and CC can be spotted in figure 4.16, which is due to the fact that longitudinal speed of vehicle with ESP only decreased within the maneuver, and thus the generated yaw rate reference used in the ESP control algorithm changed with it. Usage of ESC instead of ESP causes a significant decrease of vehicle's yaw rate overshoot. The reasons for that are that ESC is always active, unlike ESP, and that ESC uses regenerative braking, which has much faster response than a classic brake. Also, controlling each wheel torque independently in case of ESC plays an important role.

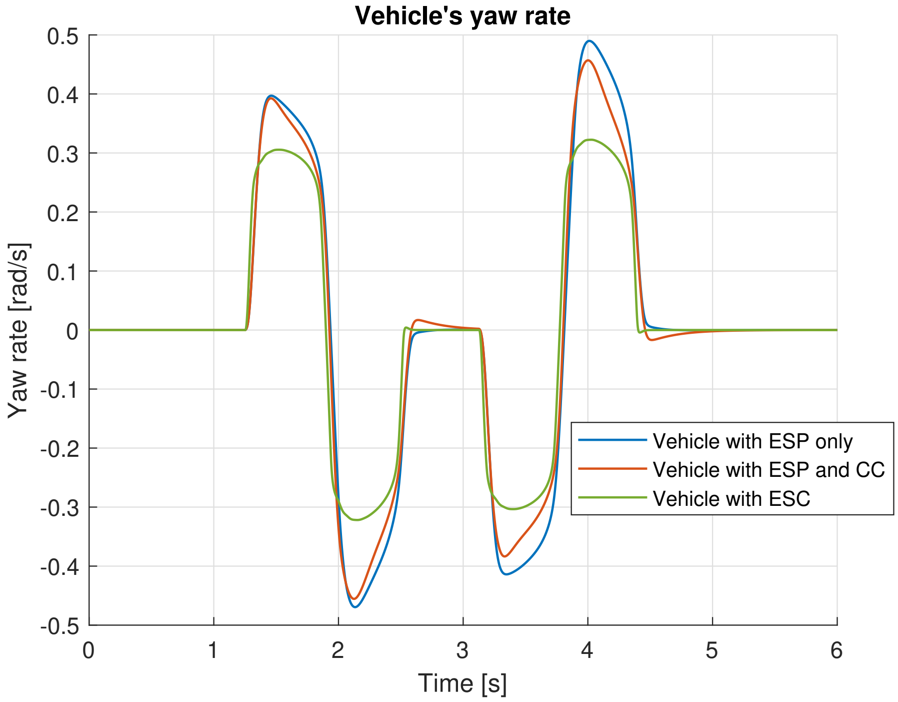

**Figure 4.16:** Vehicle's yaw rate. Comparison of vehicle with ESP only, vehicle with ESP and CC and vehicle with ESC.

Lastly, a comparison of forces acting on each tire is made. The forces in figure 4.17 are normalized, therefore the traction ellipse is turned into a unit circle. The normalized forces are

$$F_{x,N} = \frac{F_x}{F_{x,max}}, \tag{4.1}$$

$$F_{y,N} = \frac{F_y}{F_{y,max}}. \tag{4.2}$$

The figure shows distribution of forces for each wheel within the entire duration of the maneuver. Since $F_x$ can take only negative values when just ESP is used, forces acting on each tire got pretty close to the limit of tire grip at some points of the maneuver. For instance, taking a look at forces acting on the front left tire, the lowest grip margin was less than 1% at a point marked by blue cross in 4.17. When CC is added, $F_x$ can be positive as well. This causes the forces to be distributed more evenly inside the traction circle. Concerning the front left tire again, this resulted in increase in the minimal grip margin to roughly 12% at a point marked by red cross in 4.17. Distribution of forces of vehicle with ESC is similar to that of vehicle with ESP and CC, which makes further improvements of cornering performance possible, unlike vehicle with ESP only. The minimal front left tire grip margin at a point marked by green cross in 4.17 is 14%, when ESC is used.

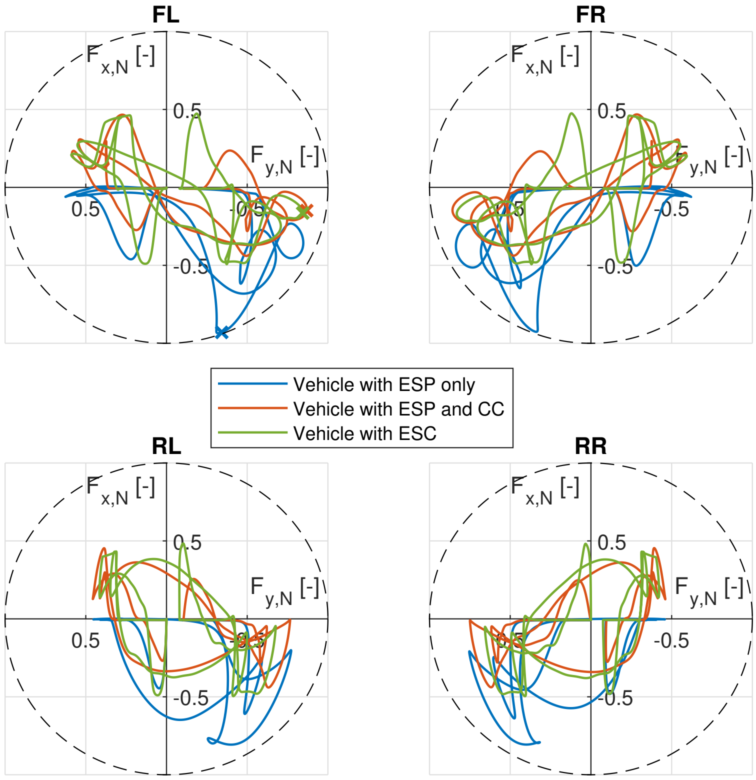

**Figure 4.17:** Forces acting on each tire. Comparison of vehicle with ESP only, vehicle with ESP and CC and vehicle with ESC.

## Chapter 5

# Conclusions

In chapter 2 derivation and implementation of vehicle models is described. In regard to the provided twin track vehicle model, the focal point of the description are the modified parts, such as actuators, external disturbances and CC, which are then validated. Additionally, reference models, namely kinematic vehicle model and model consisting of lookup tables, are presented.

Development and implementation of both stability control strategies ESP and ESC can be found in chapter 3. Both of these are linear control systems. Moreover, functionality of reference signal selector is explained in the same chapter.

The developed stabilization systems are then experimentally validated in chapter 4. Vehicle with any stability control strategy shows much better performance than uncontrolled vehicle. Furthermore, vehicle with ESC has lower yaw rate overshoot than vehicle with ESP, which means ESC performs slightly better. When only ESP is used, longitudinal speed of vehicle is not maintained and tire forces can get quite close to the tire grip limit due to their uneven distribution. To maintain longitudinal speed of vehicle and to distribute tire forces more evenly inside the traction ellipse, CC is added to work alongside with ESP. Similar improvements are achieved by using ESC instead.

# Appendix A

## Bibliography

[1] A. K. Babu. *Automotive electrical and Electronics*. Khanna Book Publishing Co. (P) Ltd., 06 2016.

[2] Vít Cibulka. Mpc based control algorithms for vehicle control. Master's thesis, Czech Technical University in Prague, 06 2019.

[3] Susan Ferguson. The effectiveness of electronic stability control in reducing real-world crashes: A literature review. *Traffic injury prevention*, 8:329–38, 01 2008.

[4] Robert Bosch GmbH. *BOSCH Automotive Handbook*. Bosch Handbooks. Robert Bosch, 2004.

[5] Mohammad Naser Hashemnia and Behzad Asaei. Comparative study of using different electric motors in the electric vehicles. pages 1 – 5, 10 2008.

[6] Jana Kukutschová, Pavel Moravec, Vladimír Tomášek, Vlastimil Matějka, Jiří Smolík, Jaroslav Schwarz, Jana Seidlerová, Klára Šafářová, and Peter Filip. On airborne nano/micro-sized wear particles released from low-metallic automotive brakes. *Environmental Pollution*, 159(4):998 – 1006, 2011.

[7] Dongbin Lu, Minggao Ouyang, Jing Gu, and Li Jianqiu. Instantaneous optimal regenerative braking control for a permanent-magnet synchronous motor in a four-wheel-drive electric vehicle. *Proceedings of the Institution of Mechanical Engineers, Part D: Journal of Automobile Engineering*, 228:894–908, 07 2014.

[8] Hans B. Pacejka and Igo J. M. Besselink. *Tire and Vehicle Dynamics*. Elsevier, 3rd edition, 2012.

[9] Philip Polack, Florent Altché, Brigitte Novel, and Arnaud de La Fortelle. The kinematic bicycle model: A consistent model for planning feasible trajectories for autonomous vehicles? pages 812–818, 06 2017.

[10] Dieter Schramm, Manfred Hiller, and Roberto Bardini. *Vehicle Dynamics*. Springer Berlin Heidelberg, 2014.

[11] Amir Masoud Soltani and Francis Assadian. New slip control system considering actuator dynamics. *SAE International Journal of Passenger Cars - Mechanical Systems*, 8, 05 2015.

# Appendix B

## Abbreviations

| | |
|---|---|
| **ABS** | Anti-lock braking system |
| **CC** | Cruise control |
| **DC** | Direct current |
| **ECU** | Electronic control unit |
| **ESC** | Enhanced stability control |
| **ESP** | Electronic stability program |
| **FL** | Front left |
| **FR** | Front right |
| **NHTSA** | National Highway Traffic Safety Administration |
| **PID** | Proportional-integral-derivative |
| **RL** | Rear left |
| **RR** | Rear right |
| **SUV** | Sport utility vehicle |
| **TCS** | Traction control system |
| **VCG** | Vehicle's center of gravity |

# Appendix C

# Nomenclature

$\alpha$ – Sideslip angle

$\beta$ – Vehicle sideslip angle

$\beta_{ref}$ – Vehicle sideslip angle reference

$\delta$ – Steering angle

$\theta$ – Pitch

$\lambda$ – Slip ratio

$\mu$ – Friction coefficient

$\rho$ – Air density

$\dot{\rho}_i$ – Angular speed of the $i$-th wheel (wheel-fixed)

$\tau$ – Time constant

$\phi$ – Roll

$\psi$ – Yaw

$\dot{\psi}$ – Yaw rate

$\dot{\psi}_{ref}$ – Yaw rate reference

$\boldsymbol{\omega}$ – Vector of angular velocity of the vehicle body (body-fixed)

$A$ – Frontal vehicle area
$C_D$ – Drag coefficient
$F_x$ – Longitudinal force
$F_{x,N}$ – Normalized longitudinal force
$F_y$ – Lateral force
$F_{y,N}$ – Normalized lateral force
$F_z$ – Normal force
$\boldsymbol{J}$ – Moment of intertia matrix
$J_i$ – Moment of inertia of $i$-th wheel
$l_f$ – Distance between VCG and front axle
$l_r$ – Distance between VCG and rear axle
$\boldsymbol{M}$ – Vector of torques
$\boldsymbol{M_{aero}}$ – Vector of external torques caused by aerodynamic forces
$M_{aero,z}$ – External yaw moment
$M_b$ – Brake torque
$M_{b,d}$ – Demanded brake torque
$M_m$ – Drive torque
$M_{m,d}$ – Demanded drive torque
$M_r$ – Regenerative braking torque
$M_{r,d}$ – Demanded regenerative braking torque
$M_z$ – Yaw moment
$P_m$ – Motor power
$r$ – Wheel radius
$\boldsymbol{r}_i$ – Position vector of the $i$-th wheel center point
$\boldsymbol{s}$ – Position vector of the vehicle body (earth-fixed)
$s$ – Complex frequency
$s_l$ – Lateral distance from VCG to left wheels
$s_r$ – Lateral distance from VCG to right wheels
$\boldsymbol{v}$ – Vector of velocity of the vehicle body (body-fixed)
$v_x$ – Longitudinal speed at the VCG
$v_{x,ref}$ – Longitudinal speed reference
$v_y$ – Lateral speed at the VCG

# Appendix D

## Lists of vehicle parameters

| **Description** | **Symbol** | **Value** | **Unit** |
|---|---|---|---|
| Vehicle mass | $m$ | 1300 | kg |
| Gravitational constant | $g$ | 9.81 | $\mathrm{m \cdot s^{-2}}$ |
| Wheel radius | $r$ | 0.33 | m |
| Moment of inertia of $i$-th wheel | $J_i$ | 1 | $\mathrm{kg \cdot m^2}$ |
| Moment of inertia along $x$-axis (body) | $J_{xx}$ | 200 | $\mathrm{kg \cdot m^2}$ |
| Moment of inertia along $y$-axis (body) | $J_{yy}$ | 1300 | $\mathrm{kg \cdot m^2}$ |
| Moment of inertia along $z$-axis (body) | $J_{zz}$ | 1400 | $\mathrm{kg \cdot m^2}$ |
| Distance between VCG and front axle | $l_f$ | 1.3725 | m |
| Distance between VCG and rear axle | $l_r$ | 1.3725 | m |
| Lateral distance from VCG to left wheels | $s_l$ | 0.85 | m |
| Lateral distance from VCG to right wheels | $s_r$ | 0.85 | m |
| Air density | $\rho$ | 1.22 | $\mathrm{kg \cdot m^{-3}}$ |
| Drag coefficient | $C_D$ | 0.18 | - |
| Frontal vehicle area | $A$ | 2 | $\mathrm{m^2}$ |
| Time constant of electric motor | $\tau_m$ | 2 | ms |
| Maximum motor power | $P_{m,max}$ | 50 | kW |
| Maximum drive torque | $M_{m,max}$ | 500 | N·m |
| Brake lag | $\tau_b$ | 20 | ms |
| Maximum brake torque | $M_{b,max}$ | 2000 | N·m |

| **Description** | **Symbol** | **Value** | **Unit** |
|---|---|---|---|
| Longitudinal stiffness factor | $B_x$ | 7 | - |
| Longitudinal shape factor | $C_x$ | 1.6 | - |
| Longitudinal peak factor | $D_x$ | 4300 | N |
| Longitudinal curvature factor | $E_x$ | $-0.5$ | - |
| Lateral stiffness factor | $B_y$ | $-8.11$ | - |
| Lateral shape factor | $C_y$ | 1.3 | - |
| Lateral peak factor | $D_y$ | 3900 | N |
| Lateral curvature factor | $E_y$ | 0.2 | - |